Neurotoxicology 97 (2023) 65–77

Contents lists available at ScienceDirect

Neurotoxicology

journal homepage: www.elsevier.com/locate/neuro

Evaluation of mRNA markers in differentiating human SH-SY5Y cells for estimation of developmental neurotoxicity

M.G. Hinojosa [a,1], Y. Johansson [a,1], A. Cediel-Ulloa [b], E. Ivanova [a], N. Gabring [a], A. Gliga [c], A. Forsby [a,*]

[a] Department of Biochemistry and Biophysics, Stockholm University, 106 91 Stockholm, Sweden
[b] Department of Organismal Biology, Environmental Toxicology, Uppsala University, 752 36 Uppsala, Sweden
[c] Institute of Environmental Medicine, Karolinska Institute, 171 77 Stockholm, Sweden

ARTICLE INFO

Edited by Harm J. Heusinkveld

Keywords:
Developmental neurotoxicity
in vitro
mRNA markers
Live-cell imaging
Neurite outgrowth

ABSTRACT

Current guidelines for developmental neurotoxicity (DNT) evaluation are based on animal models. These have limitations so more relevant, efficient and robust approaches for DNT assessment are needed. We have used the human SH-SY5Y neuroblastoma cell model to evaluate a panel of 93 mRNA markers that are frequent in Neuronal diseases and functional annotations and also differentially expressed during retinoic acid-induced differentiation in the cell model. Rotenone, valproic acid (VPA), acrylamide (ACR) and methylmercury chloride (MeHg) were used as DNT positive compounds. Tolbutamide, D-mannitol and clofibrate were used as DNT negative compounds. To determine concentrations for exposure for gene expression analysis, we developed a pipeline for neurite outgrowth assessment by live-cell imaging. In addition, cell viability was measured by the resazurin assay. Gene expression was analyzed by RT-qPCR after 6 days of exposure during differentiation to concentrations of the DNT positive compounds that affected neurite outgrowth, but with no or minimal effect on cell viability. Methylmercury affected cell viability at lower concentrations than neurite outgrowth, hence the cells were exposed with the highest non-cytotoxic concentration. Rotenone (7.3 nM) induced 32 differentially expressed genes (DEGs), ACR (70 μM) 8 DEGs, and VPA (75 μM) 16 DEGs. No individual genes were significantly dysregulated by all 3 DNT positive compounds ($p < 0.05$), but 9 genes were differentially expressed by 2 of them. Methylmercury (0.8 nM) was used to validate the 9 DEGs. The expression of *SEMA5A* (encoding semaphorin 5A) and *CHRNA7* (encoding nicotinic acetylcholine receptor subunit α7) was downregulated by all 4 DNT positive compounds. None of the DNT negative compounds dysregulated any of the 9 DEGs in common for the DNT positive compounds. We suggest that *SEMA5A* or *CHRNA7* should be further evaluated as biomarkers for DNT studies *in vitro* since they also are involved in neurodevelopmental adverse outcomes in humans.

1. Introduction

The number of children being diagnosed with neurodevelopmental disabilities has increased over the past decades (Boyle et al., 2011; Zablotsky et al., 2019). One reason for this increase may be related to chemical exposure during pregnancy (National Research Council, 2000; Grandjean and Landrigan, 2006). Developmental neurotoxicity can be defined as an adverse alteration in the function and structure of the developing nervous system caused by chemical exposure during pregnancy (Aschner et al., 2017). Neuronal development starts as early as 2 weeks after gestation with a highly controlled and structured timeframe and coordination of molecular and cellular events that arguably

Abbreviations: ACR, Acrylamide; ADHD, Attention deficit hyperactivity disorder; AOP, Adverse outcome pathway; ASD, Autism spectrum disorder; BDNF, Brain derived neurotrophic factor; CREB, cAMP responsive element-binding protein; DEG, Differentially expressed gene; DNT, Developmental neurotoxicity; EC_{20}, The estimated concentration giving 20% effect; FC, Fold change; FDR, False discovery rate; GDF15, Growth differentiation factor 15; HDAC, Histone deacetylase; hESC, Human embryonic stem cell; IPA, Ingenuity Pathway Analysis; KE, Key event; MeHg, Methylmercury chloride; nAChR, Nicotinic acetylcholine receptor; NAMs, New approach methods; NPC, Neural progenitor cells; PBS, Phosphate buffered saline; PenStrep, Penicillin/streptomycin; RA, all-trans retinoic acid; SEMA5A, Semaphorin 5A; VPA, Valproic acid.

* Corresponding author.
E-mail address: anna.forsby@dbb.su.se (A. Forsby).
[1] Both authors contributed equally

https://doi.org/10.1016/j.neuro.2023.05.011
Received 13 January 2023; Received in revised form 5 May 2023; Accepted 17 May 2023
Available online 18 May 2023

continues throughout the lifespan. Thus, the developing brain is highly sensitive to chemical exposure and the timepoint of exposure may lead to different adverse outcomes, depending on the crucial event taking place at the particular developmental stage. In this sense, the moment of the exposure is relevant, as exposure in the first trimester of pregnancy can lead to abnormalities on the brain and spinal cord that might even lead to abortion (Rice and Barone, 2000). In addition, several chemicals are known to cross the placenta, depending on their physicochemical characteristics and, consequently, increase fetal exposure (Myren et al., 2007). Therefore, there is an emerging need to screen chemicals for DNT assessment.

There are about 86,000 chemicals registered for commercial use in the USA (EPA, 2022) and more than 21,000 chemicals registered under the Registration, Evaluation, Authorization and Restriction of Chemicals (REACH) in Europe (ECHA, 2018). Despite the large number of chemicals on the market, only about 200 chemicals have been tested for DNT according to regulatory guidelines (Martin et al., 2022). The current DNT test guidelines, that were established by the Organization for Economic Co-operation and Development (OECD TG426) and by the Environmental Protection Agency (EPA) (OPPTS 870.6300) are entirely based on *in vivo* experiments, which are time-consuming, expensive, and require many animals, i.e. factors that limit the screening of compounds (EPA, 1998; OECD, 2007). New approach methodologies (NAMs), including *in vitro* and *in silico* methods, can provide useful and more relevant information for human DNT risk assessment and regulatory decision-making (Crofton et al., 2014; Fritsche et al., 2017; Sachana et al., 2021). Established *in vitro* test batteries are not only cheaper and faster but can also enable investigations on key neurodevelopmental processes (Masjosthusmann et al., 2020). Such tests may include studies on proliferation, migration, neural differentiation, neurite outgrowth, synapse formation and function and neuroinflammation, as well as other cellular endpoints such as, epigenetics, apoptosis, oxidative stress and energy metabolism (Aschner et al., 2017; Bal-Price et al., 2018b; Fritsche et al., 2015). In addition, toxicogenomics is a useful tool to identify mRNA biomarkers that are important for neuronal development (Attoff et al., 2017; de Leeuw et al., 2022; Hogberg et al., 2010; Krug et al., 2013). The number of relevant alternative cell models for DNT studies has increased, including neuronal progenitor cells derived from primary tissue, human embryonic stem cell (hESC) lines, human induced pluripotent stem (iPS) cell lines, as well as human neuronal cell lines (e.g. Koch et al., 2022; Krug et al., 2013; Martínez et al., 2020; Schwartz et al., 2015).

The objective of this study was to evaluate mRNA markers that are important for neuronal development *in vitro* by using the human neuroblastoma SH-SY5Y cell model. By exposing these cells to chemicals during 6 days of retinoic acid (RA)-induced differentiation, we aimed to identify a set of genes that can be used as biomarkers for *in vitro* DNT screening. In addition, we developed a method for assessment of neurite outgrowth by live-cell fluorescence imaging and a pipeline for automatic image analysis. Four well-known DNT-positive and 3 DNT-negative chemicals were selected for test method evaluation. The choice of test compounds was based on their different molecular targets and diverse modes of action in humans or in animal models. The crop protection chemical and mitochondrial complex I inhibitor rotenone, the antiepileptic, antimigraine and mood stabilizing pharmaceutical and histone deacetylase (HDAC) inhibitor valproic acid (VPA), and the environmental and food pollutants and electrophilic chemicals acrylamide (ACR) and methylmercury (MeHg) were used as positive compounds (Aaseth et al., 2020; Fathe et al., 2014; LoPachin et al., 2007; Schmitz et al., 2021). Three chemicals with no known effect on the developing nervous system were used as negative compounds; tolbutamide (antidiabetic drug), clofibrate (controlling blood lipids), and D-mannitol (diuretic with poor intestinal uptake) (Krebs et al., 2020; Martin et al., 2022).

2. Materials and methods

2.1. Materials

For information, see Supplementary 1 Table S1. Information concerning the compounds tested can be found in Supplementary 1 Table S2.

2.2. Cell culture

Human neuroblastoma SH-SY5Y cells (used between passage number 50–70) were cultured as previously described (Attoff et al., 2016), and screened for mycoplasma contamination bi-monthly. The cells were cultured in minimum essential medium (MEM) supplemented with 10% fetal bovine serum (FBS), 2 mM L-glutamine, non-essential amino acids (added according to the supplier's recommendations), 100 μg/mL streptomycin and 100 U/mL penicillin (PenStrep). For routine culture, SH-SY5Y cells were passaged once a week using TrypLE Express Enzyme and seeded in 75 cm^2 cell culture flasks at 27,000 cells/cm^2 and the medium was changed after 3 days. For differentiation studies, the SH-SY5Y cells were seeded in routine culture medium at 12,500 cells/cm^2. After 24 h, the medium was exchanged to differentiation medium consisting of Dulbecco's Modified Eagle's Medium/Nutrient Mixture F-12 Ham (DMEM/F12) supplemented with PenStrep, 1 mM L-glutamine, N2 supplement (added according to the supplier's recommendations), and 1 μM RA. The cells were incubated in a humidified CO_2 (5%) incubator at 37 °C. All cell culture media and supplements were purchased from Gibco except for RA that was purchased from Merck (see Supplementary Table S1 for details).

2.3. Exposure

All information about the tested compounds, solvents and concentrations are listed in Supplementary 1 Table S2. Stock solutions of rotenone and methylmercury (II) chloride were prepared in dimethyl sulfoxide (DMSO) and stored in aliquots at − 20℃, while the aliquots of tolbutamide and clofibrate were freshly prepared in DMSO prior use. The final concentration of DMSO in the control and exposed cells was adjusted to 0.1%. Acrylamide, valproic acid sodium salt and D-mannitol, were freshly dissolved in DMEM/F12 supplemented with PenStrep and L-glutamine followed by filter sterilization for each experiment. The final concentrations were then prepared in complete differentiation medium. The scheme for exposure and differentiation is illustrated in Fig. 1. All cell culture media and supplements were purchased from Gibco except for DMSO that was purchased from Merck (see Supplementary Table S1 for details).

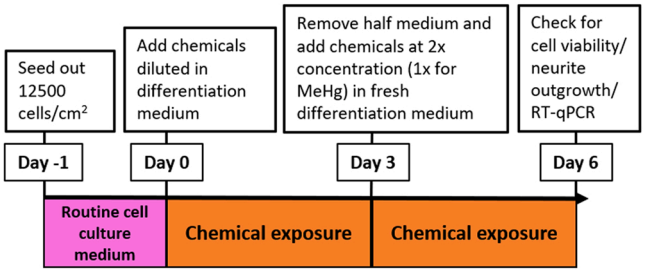

Fig. 1. Overview of the experimental set up for studying cell viability, neurite outgrowth and mRNA expression after 6 days of differentiation and chemical exposure in SH-SY5Y cells. For cell viability and neurite outgrowth, cells were seeded in 96-well plates and in 60 mm petri dishes for RT-qPCR. At day 3, the cells were exposed to 1x concentration of MeHg since no elimination from the cell culture was expected, which may be possible for the other compounds (however not measured).

2.4. Cell viability

The resazurin assay was used to determine the metabolic activity, reflecting the amount of viable cells after exposure (O'Brien et al., 2000). A 20x solution was prepared by dissolving resazurin sodium salt (Merck) in phosphate buffered saline (PBS), and 0.1 M NaOH. The stock solution was filter sterilized and stored at 4 °C protected from light. The experimental set up is illustrated in Fig. 1. SH-SY5Y cells were seeded in clear 96-well plates at 12,500 cells/cm^2 in 100 μL. After 24 h, the exposure and differentiation were initiated by exchanging the medium to 100 μL of chemicals diluted in differentiation medium (Supplementary 1 Table S2). The medium was changed after 3 days by removing 50 μL from each well, followed by addition of 50 μL fresh medium containing 2x concentration of test compounds except for MeHg, which was 1x since no elimination of MeHg from the cell culture was expected (Morel et al., 1998). The choice of adding 50 μL 2x concentration in 50 μL old exposure medium was based on the assumption that the free concentrations of the test compounds decrease during exposure because of e.g. conjugation to glutathione and other macromolecules in the cell system, binding of highly lipophilic compounds to the plastic and β-oxidation in the mitochondria (Fennell and Friedman, 2005; Galasko, 2017; Methaneethorn, 2018; Proença et al., 2021; Rozman et al., 2010). After another 3 days of exposure and differentiation, 50 μL from each well were removed and 50 μL of 2x resazurin solution were added followed by 2 h incubation at 37 °C and 5% CO_2. Resorufin fluorescence was then measured from the top at excitation 540 nm and emission 590 nm using a SpectraMax M2E (Molecular Devices, USA).

2.5. Neurite outgrowth

Live-cell imaging was performed in black 96-well plates with μ-clear bottom (Greiner) that were pre-coated with 1 μg/mL poly-D-lysine dissolved in sterile water, using the same cell seeding density, differentiation, and exposure procedure as for cell viability explained in 2.4 (Fig. 1). The concentrations used were adjusted, based on the cell viability results (Supplementary 1 Table S2). After 6 days of differentiation and exposure, the cells were stained by adding 20 μL of 1 μM calcein-AM and 1 μM Hoechst-33342 to each well without removing the exposure medium, followed by a 20 min incubation at 37 °C and 5% CO_2 to allow for full hydrolysis of the AM group from calcein. Both calcein-AM and Hoechst-33342 were purchased from Invitrogen. Before imaging, 130 μL of fresh DMEM/F12 were added to each well to dilute extracellular calcein-AM. The fluorescence of intracellular calcein and Hoechst-33342 was imaged at 6 positions per well in an inverted ZEISS Axio Observer 7 widefield microscope (Carl Zeiss Microscopy BmbH, Jena, Germany) equipped with an ORCA-Fusion CMOS camera (C15440–20OP, Hamamatsu Photonics, Japan), using a Plan-Apochromat 20x/0.8 M27 objective. Images were depicted for 50 ms exposure time in 2 channels using a 405/493/575/654/761 beam splitter. Calcein in channel 1 was detected at 488 nm_{em}/520 nm_{ex} (for GFP) and Hoechst-33342 in channel 2 was detected at 361 nm_{em}/497 nm_{ex} (for DAPI) using the ZEN Blue 3.1 software. CellProfiler version 3.1.9 was used for quantitative image analysis. Neurite outgrowth was defined on a population basis at a ratio of total neurite area (stained by calcein-AM) to total nuclei area (stained by Hoechst-33342) per imaged field. In order to enhance the neurite pixels, the "Speckles" algorithm was used that identified objects based on size and intensity. The total area of neurite objects was then divided by the total area of nuclei objects. The CellProfiler pipeline is available in the Supplementary file 2.

2.6. RNA extraction and cDNA synthesis

Cells were seeded in 60 mm in diameter dishes at a density of 12,500 cells/cm^2 in 5 mL routine culture medium. Twenty-four hours after seeding, the routine culture medium was removed and replaced with differentiation medium containing the chemical to be tested (Fig. 1). The concentrations used were based on the results from the neurite outgrowth and cell viability assays: rotenone, 7.3 nM; VPA, 75 μM; ACR, 70 μM; MeHg, 0.8 nM; clofibrate, 200 μM; D-mannitol, 1 mM and tolbutamide, 100 μM (Supplementary 1 Table S2).

After 3 days of exposure, half of the medium was removed and 2.5 mL of a freshly prepared 2x concentration (1x for MeHg) solution in differentiation medium was added, assuming some elimination of the free concentrations during the exposure (see Section 2.4). After totally 6 days of exposure, the medium was removed and the cells were washed with 5 mL PBS and then detached with 1 mL TrypLE Express Enzyme for 2 min at 37 °C. The cells were resuspended in 4 mL routine culture medium and then put in a 15 mL centrifuge tube followed by centrifugation for 5 min at 300 g. The supernatant was removed, and the pellets were stored at − 80 °C until RNA extraction. The RNA extraction was performed using the RNAeasy Plus Mini kit according to the manufacturer's instructions (Qiagen). mRNA concentration was determined using a NanoPhotometer P-class (Implen GmbH). One μg of RNA was used to prepare matching cDNA by using the iScript cDNA synthesis Kit (Bio-Rad). The cDNA was subsequently diluted to 10 ng/uL in RNAse free water and stored at − 80 °C. The quality of each sample was assessed using experimental control assays for genomic DNA (PrimePCR DNA Contamination Control SYBR Green Assay), reverse transcription (PrimePCR Reverse Transcription Control SYBR Green Assay), RNA quality (PrimePCR RNA Quality SYBR Green Assay) and PCR performance (PrimePCR Positive Control SYBR Green Assay). All quality control primers were purchased from Bio-Rad. The quality control reactions were performed in an iQ5 Real-Time PCR Detection System (Bio-Rad) using SsoAdvanced Universal SYBR Green Supermix.

2.7. Selection of mRNA markers important for neurodevelopment

In 2020, we published a study in which the whole cell transcriptome was determined by RNA-sequencing in SH-SY5Y cells after 3, 6 and 9 days of RA-induced differentiation. Differentially expressed genes (DEGs) were identified by using the DESeq2 package in Bioconductor (Attoff et al., 2020). The raw RNA-sequencing data have been deposited at European Nucleotide Archive (ENA) (accession ID: PRJEB23591). Downstream analyses were carried out with the use of QIAGEN Ingenuity Pathway Analysis (IPA), a commercially available software that can analyze big gene expression pattern. Compared to other gene enrichment analysis tools available, IPA is continuously curated with scientific-based observed data (Krämer et al., 2014). Core analyses with the adjusted p-value ≤ 0.05 cut off limits were executed in order to identify DEGs at days 3, 6 and 9 of RA-induced differentiation. The DEGs were then annotated in IPA and a cutoff on the absolute log2 fold change (FC) > 1 was set. These analyses culminated with the final identification of 2017 DEGs for the comparison of days 3 vs day 0, 3219 DEGs for the comparison of day 6 vs day 0, and 3726 DEGs for the comparison day 9 vs day 0. A Venn diagram of the obtained data revealed a total of 1753 common DEGs between days 3, 6 and 9 of RA-induced differentiation (Fig. 2). These 1753 common DEGs were subsequently used for canonical pathway analysis and resulted in 238 DEGs that were part of the "Neurotransmitters and others canonical pathway". Next, an overlay between our 238 DEGs and 55 annotations part of "Diseases and Functions related to nervous system" available in IPA (Supplementary 1 Table S3) was carried out. The 238 DEGs were ranked based on the frequency of appearance in the 55 annotations (Supplementary file 3) using a script written in Python version 3.10.5 (Supplementary file 4).

The final list resulted in 95 genes including 2 housekeeping genes, used for normalization, to fit 4 samples on one 384 well primePCR plate (see below and Supplementary 1 Fig. S2. The 93 genes selected included 7 genes added based on relevance for DNT and interest from previous research. Therefore, the top 86 genes from the IPA analysis were selected and the mean raw counts were checked for each gene after 6 days of differentiation from RNA-seq data. All genes below mean 20

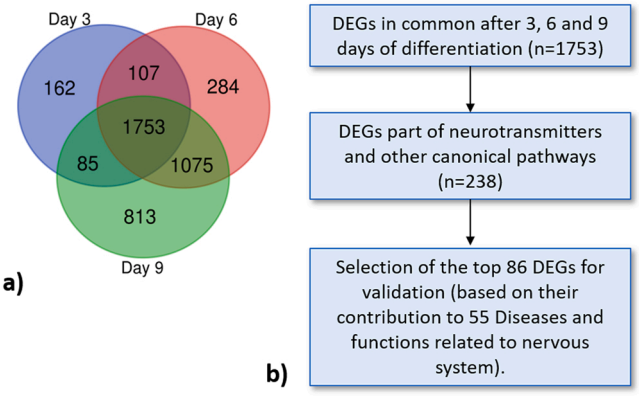

Fig. 2. Identification of DEGs used as markers of DNT a) Venn diagram indicating the common DEGs expressed in SH-SY5Y cells during 3, 6 and 9 days of RA-induced differentiation b) Flow chart illustrating the selection of 89 markers that are important for neuronal development and expressed in 3, 6, and 9 days -differentiated SH-SY5Y cells. The selection was performed using IPA software.

counts were removed because of low read out probability after exposure to chemicals and the next gene on the list was subsequently added and the mean counts were checked. The additional 7 genes were selected, based on the following conditions. Both mRNA and protein expression of brain derived neurotrophic factor (BDNF) and cAMP response element-binding protein 1 (CREB1) were previously investigated in SH-SY5Y cells that were exposed to ACR during 9 days of differentiation (Attoff et al., 2020). CYP26A1 metabolizes RA, which was used to differentiate the SH-SY5Y, and is of importance for neuronal patterning and differentiation (Langton and Gudas, 2008; Uehara et al., 2007). Growth associated protein 43 (GAP43), also referred to as 'growth' or 'plasticity' protein, was chosen since it is highly expressed during neuronal development, axonal outgrowth and regeneration (McGuire et al., 1988; Widmer and Caroni, 1990). Growth differentiation factor 15 (GDF15) is used as a clinical marker for disease progression, such as Alzheimer's and Parkinson's disease, and cellular stress, and has been shown to promote neuroprotection in embryonic midbrain dopaminergic rat neurons (Jiang et al., 2021; Strelau et al., 2000). In addition, GDF15 has been shown to regulate proliferation and migration in the developing hippocampus in mice (Carrillo-García et al., 2014). Dysregulation and polymorphism of *CHRNA7,* the gene expressing the α7 nicotinic acetylcholine receptor (nAChR) subunit, have been associated with ASD (Bacchelli et al., 2015; Yasui et al., 2011). Nuclear receptor subfamily 3 group C member 1 (*NR3C1*) encodes for the glucocorticoid receptor, and its genetic variation has been associated with attention deficit hyperactivity disorder (ADHD) pathogenesis and cortical brain volumes (Bandeira et al., 2021). Description about each protein coding gene is listed in Supplementary 1 Table S4.

2.8. Quantitative reverse transcription polymerase chain reaction

The effects of rotenone, VPA, ACR, tolbutamide, mannitol, and clofibrate on the 95 selected genes, including 2 housekeeping genes, were analyzed using RT-qPCR. Primer pre-casted white 384-well plates were designed and purchased from Bio-Rad (see Supplementary 1 Table S4 for specific primer details and Supplementary 1 Fig. S2 for plate design). Ten ng of cDNA in 10 μL was added to each reaction according to the Bio-Rad PrimePCR instruction manual. On each 384-well plate, 2 biological replicates including control and treated samples were added. The reactions were performed using a CFX384 Real-Time PCR Detection System (Bio-Rad) using SsoAdvanced Universal SYBR Green Supermix. For MeHg, the 9 overlapping DEGs between rotenone, VPA and ACR were purchased as mono-primers from Bio-Rad. The qPCR of MeHg exposed cells was assessed in a well in a clear semi-skirted 96-well plate with 10 ng of cDNA in a total volume of 20 μL containing the primer and SsoAdvanced Universal SYBR Green Supermix per reaction by using an iQ5 Real-Time PCR Detection System (Bio-Rad). Raw data were analyzed using Microsoft Excel. Each gene in all samples were normalized against 2 housekeeping genes: heat shock protein 90ab (HSP90AB1) and ribosomal protein large P1 (RPLP1) which have previously been identified to be stably expressed during 3, 6 and 9 days of differentiation (Attoff et al., 2020). The cycle of quantification (Cq) for each gene was subtracted with the mean Cq of the 2 housekeeping genes in each sample, referred to as ΔCq. Relative fold change (FC) expression for each gene was calculated subtracting the ΔCq of the treated sample with the ΔCq of the corresponding control sample, referred to as ΔΔCq, and was further calculated by taking 2 to the power of negative ΔΔCq, i.e. $2^{-\Delta\Delta Cq}$ (Livak et al., 2013).

2.9. Data analysis

GraphPad Prism 9.2.0 was used for statistical analysis of the data. For the curve fit analysis of the cell viability and neurite outgrowth results, the values were normalized, setting 0% as Y= 0, and the negative control (cells exposed to only vehicle) to 100%. After this, the dose-response curve was set as log(inhibitor) vs. response with variable slope, setting the constants top = 100 and bottom = 0. The results of the experiments were analyzed by interpolating the concentration giving 20% effect (EC_{20}, i.e. X at Y=80) from the curves obtained. Cell viability and neurite outgrowth results were analyzed against control samples set to 100%, by using the non-parametric, uncorrected Dunn's multiple comparisons test followed by the Kruskal-Wallis test, assuming non-gaussian distribution of the control group and un-equal SD in groups. When EC_{20} for neurite outgrowth did not differ from the EC_{20} for cell viability, the approximate highest non-cytotoxic concentration was estimated. RT-qPCR results were analyzed using paired parametric multiple t-test comparing the treated ΔCq values with control ΔCq values with a p-value set to 5%. Input data for all heatmaps are presented as log2 FC expression. The venn diagram was created using the VennDiagram package running in RStudio version 1.1.456. All data are deposited at https://su.drive.sunet.se/index.php/s/axn6QqnLmAoX24K.

3. Results

3.1. Neurite outgrowth and cell viability

Developmental neurotoxicity endpoints should be assessable at non-cytotoxic concentrations. Here, we developed a protocol for assessment of neurite outgrowth in live cells by using high content fluorescence imaging and an automated protocol for image analysis (Fig. 3). Neurite outgrowth was analyzed as a DNT endpoint, and the objective was to choose a concentration of each compound for gene expression analysis that attenuated neurite outgrowth but was not affecting cell viability. To assess these endpoints, SH-SY5Y cells were exposed to each compound in a wide range of concentrations during 6 days of differentiation, where after neurite outgrowth and cell viability were determined (Fig. 4). The concentrations for further studies on gene expression were chosen from the concentration-effect curves.

Rotenone impaired neurite outgrowth at 33 nM and higher concentrations, but did not alter cell viability significantly up to 100 nM. At 10 μM 100% cell death was induced after 6 days of exposure (Fig. 4a). The EC_{20} for rotenone, at which 20% reduction in neurite outgrowth was estimated, was determined to 7.3 nM and used to expose for gene expression analysis. Furthermore, VPA attenuated neurite outgrowth significantly at 254 μM and with no statistically significant effect on cell viability until 660 μM and higher (Fig. 4c). As there was a slight decrease in neurite outgrowth at 9–85 μM and non-significant decrease in viability at 100 μM, we used 75 μM as the approximate highest concentration affecting neurite outgrowth but not cell viability for gene expression analysis. Concerning MeHg, the cell viability was affected at a slightly lower concentration than the concentration that attenuated

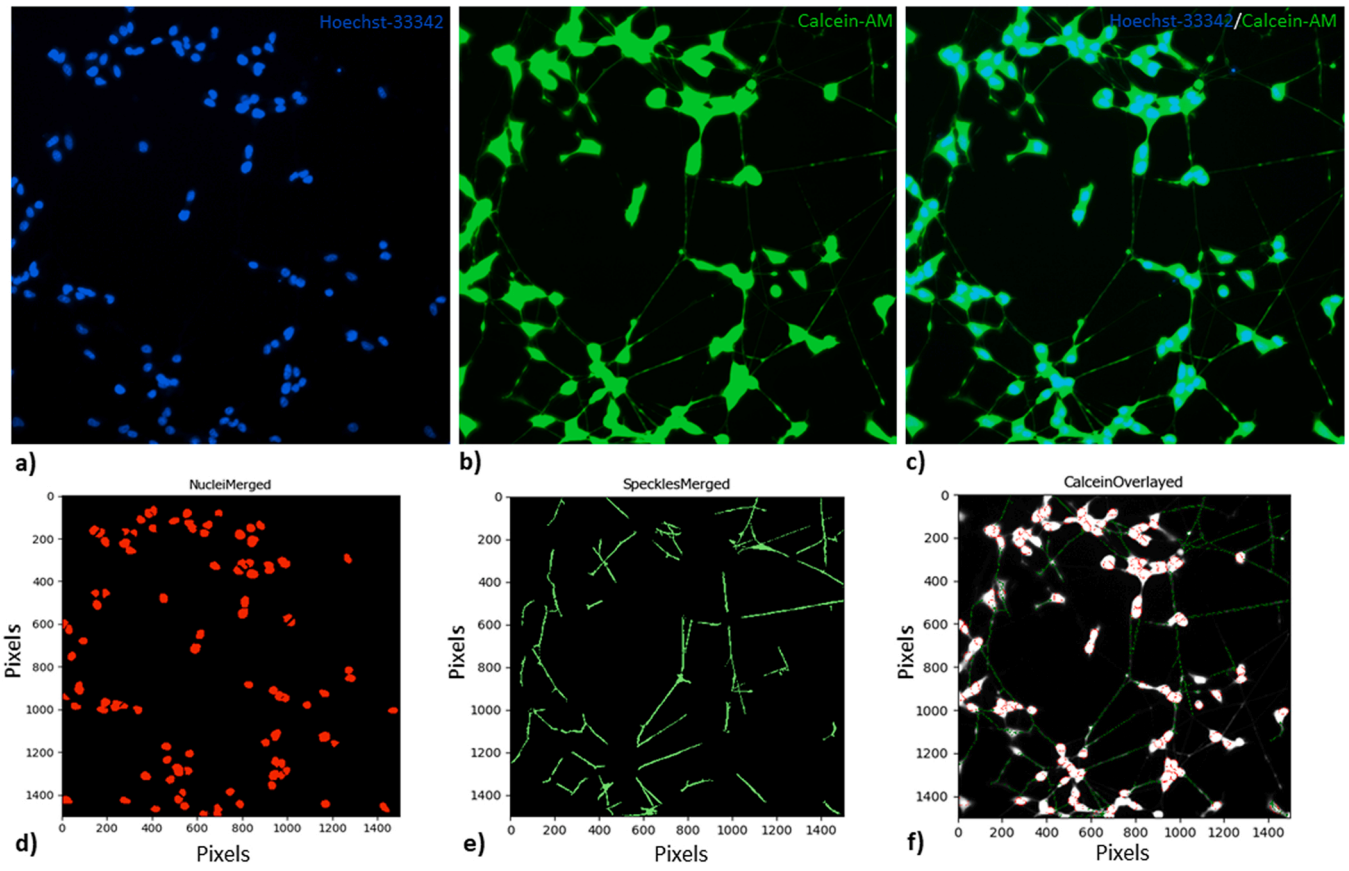

Fig. 3. Automated neurite outgrowth analysis using CellProfiler. SH-SY5Y cells were stained with Hoechst-33342 (a) and calcein-AM (b), overlay in (c), after 6 days of differentiation and exposure. The pixel area of total nuclear staining (d) and speckles (neurites) (e, f) were identified and quantified in CellProfiler. The data were analyzed by taking the total pixel area speckles over total pixel area nuceli. The images are representative of a control sample (cells cultured in differentiation medium).

neurite outgrowth after 6 days of exposure (Fig. 4e). Hence, the highest non-cytotoxic concentration, 0.8 nM, was used for the gene expression analysis. The 2 DNT-negative compounds clofibrate and tolbutamide did neither show effect on neurite outgrowth, nor on cell viability (Fig. 4b and f). Hence, the highest concentrations tested for both compounds were used for the exposure for gene expression analysis. D-mannitol decreased the cell viability significantly at 0.1 M and 0.5 M (Fig. 4d). The highest, non-cytotoxic concentration 1 mM was selected for gene expression analysis. All concentrations used for exposure in the transcriptomic analyses are listed in Table 1.

3.2. RNA sequencing analysis of differentiated SH-SY5Y cells identified markers for neuronal development

Differentiated human neuroblastoma SH-SY5Y cells were used as a model for neuronal development. We performed a new pathway and network analysis on genes that were differentially expressed in SH-SY5Y cells during 3, 6 and 9 days of differentiation from previous published RNA-sequencing data (Attoff et al., 2020). From the IPA analysis a final selection of 86 genes were made, based on the number of annotations relevant to neuronal function that each gene was involved in, ranked from occurrence in 51 of 55 annotations (*NTRK2*) to 12 annotations (*SLIT1*) (Supplementary file 3 and Supplementary 1 Fig. S1). The expression of the 86 most annotated genes on day 3, 6 and 9 in relation to undifferentiated SH-SY5Y cells, together with the expression of 7 additional genes that are relevant for DNT, is presented as log2 FC in alphabetical order in Fig. 5.

3.3. The expression of selected biomarkers was dysregulated by known neurotoxic compounds

In order to evaluate the selected genes as potential biomarkers for DNT, their expression was analyzed after exposure of the differentiating SH-SY5Y cells with rotenone, VPA and ACR (positive for DNT) and 3 DNT negative compounds (clofibrate, D-mannitol and tolbutamide) at non-cytotoxic concentrations. After exposure for 6 days during differentiation, the cells were harvested and the selected markers were investigated using RT-qPCR. Rotenone significantly altered the expression of 32 genes (11 upregulated and 21 downregulated) ($p < 0.05$) whilst VPA dysregulated 16 (4 upregulated and 12 downregulated) and ACR 8 genes (all downregulated), respectively. Surprisingly, the negative compounds also dysregulated a few genes; 3 genes were downregulated by tolbutamide, 1 upregulated by clofibrate and 4 downregulated by D-mannitol (Fig. 6).

An overlap analysis of the DEGs ($p < 0.05$) shows that there was no overlap in DEGs between all the 3 positive compounds (Fig. 6c). However, *TP53* (encoding the transcription factor tumor protein 53), *NTRK1* (encoding neurotrophic tyrosine kinase receptor 1), *NRXN1* (encoding neurexin 1), *DPYSL3* (encoding dihydropyrimidinase like 3), *EDNRA* (encoding endothelin receptor type A) and *CHRNA7* were dysregulated by both rotenone and VPA whilst *CNR1* (encoding cannabinoid receptor 1) and *SEMA5A* (encoding semaphorin 5A) were in common between VPA and ACR and *OPRD1* (encoding opioid receptor delta 1) was in common for rotenone and ACR. There were thus 9 DEGs identified that may be useful as future DNT markers.

The 9 DEGs that were shared between 2 of the positive compounds (rotenone, VPA or ACR) were validated in another qPCR set-up after

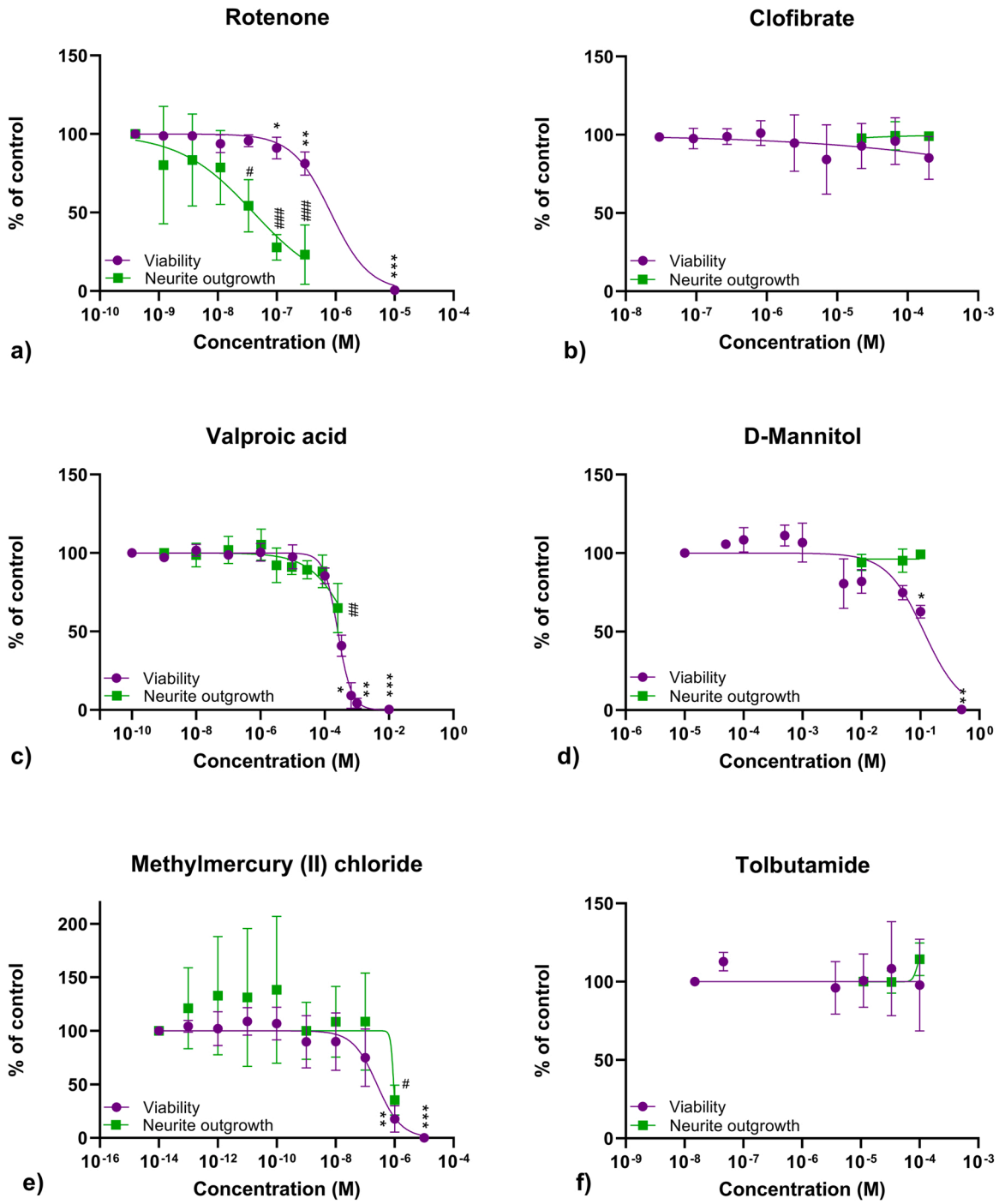

Fig. 4. Cell viability and neurite outgrowth after 6 days of exposure during differentiation in SH-SY5Y cells. Cells were exposed to the positive compounds a) rotenone c) valproic acid e) methylmercury (II) chloride and the negative compounds b) clofibrate d) D-mannitol e) tolbutamide. The data are presented as the mean of 2–6 biological replicates, each performed in 5–6 technical replicates. The results were analyzed using the non-parametric Kruskal-Wallis multiple comparison test. The bars represent the mean ±SD. *p < 0.05, **p < 0.01, ***p < 0.001 cell viability, #p < 0.05, ##p < 0.01, ###p < 0.001 neurite outgrowth, both in comparison to negative controls, set to 100%.

exposure with MeHg, which is referred to as the 'gold standard' DNT-positive compound. The gene expression of MeHg-exposed SH-SY5Y cells were analyzed using single (mono)-primer quantitative RT-PCR (Fig. 7).

The 4 DNT-positive compounds downregulated *CHRNA7, DPYSL3, NTRK1, OPRD1, SEMA5A* and *TP53*, however not all statistically significantly. *EDNRA* was downregulated after MeHg exposure whilst being upregulated by the other compounds. *NRXN1* was downregulated by VPA and ACR, but was not altered by rotenone and MeHg. Also, MeHg and rotenone downregulated *CNR1* but was upregulated after VPA exposure and not affected by ACR (Fig. 7). The dysregulation observed after MeHg exposure did not show any statistically significant up- or downregulation, which can be explained by the fact that only 2 biological replicates were tested. However, the downregulation of 6 of the genes were consistent between all compounds.

Table 1
Concentrations used for gene expression analyses and the criteria for concentration selection.

Compound	Concentration	Criteria
Rotenone	7.3 nM	EC_{20} affecting neurite outgrowth
Valproic acid	75 μM	Approximate highest non-cytotoxic concentration found in this study.
Acrylamide[a]	70 μM	Previously determined highest non-cytotoxic concentration, which significantly attenuated neurite outgrowth by approximately 40% (Attoff et al., 2016; Attoff et al., 2020).
Methylmercury (II) chloride	0.8 nM	Approximate highest non-cytotoxic concentration found in this study.
Clofibrate	200 μM	Highest concentration tested, considered solubility features. Did neither change cell viability, nor neurite outgrowth.
D-mannitol	1 mM	Highest concentration that did neither affect cell viability, nor neurite outgrowth.
Tolbutamide	100 μM	Highest concentration tested, considered solubility features. Did neither change cell viability, nor neurite outgrowth.

[a] Not tested by live cell imaging or cell viability in this study.

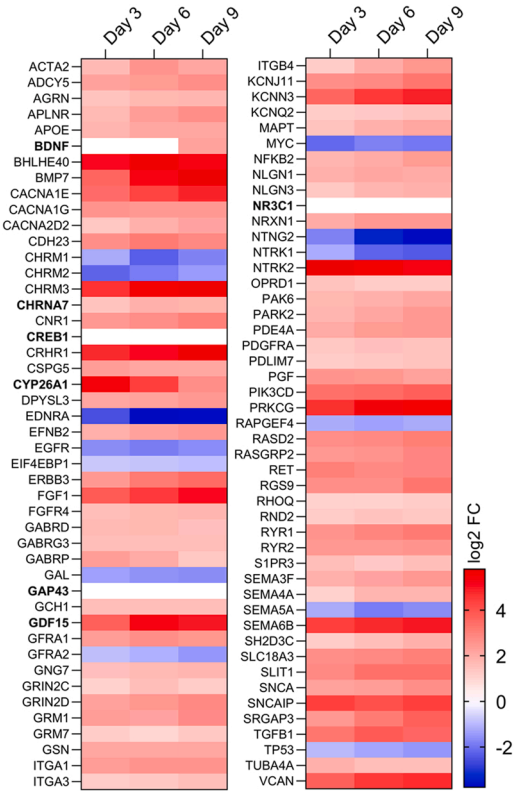

Fig. 5. Mapping of the final set of 93 differentially expressed genes (DEGs) during retinoic acid induced differentiation of SH-SY5Y cells. Heatmap of the 93 selected genes showing the differential expression after 3, 6 and 9 days of differentiation in relation to undifferentiated cells (day 0). The 86 genes that were top ranked in number of occurrences in the annotation part of diseases and functions related to nervous system, based on RNAseq data and IPA analysis, and 7 genes (bold) selected based on previous research. Color coding refers to the log2 FC expression.

4. Discussion

To overcome the large number of animals, the cost and long time to perform a regulatory DNT study, well-established and robust NAMs, such as cell-based *in vitro* test assays and *in silico* modeling can to be considered for DNT screening (Bal-Price et al., 2018a; Fritsche et al., 2018a, 2018b; Smirnova et al., 2014). Here we used the human neuroblastoma SH-SY5Y cell line as a model for immature neurons, resembling neuroblasts at an early gestational stage (Budday et al., 2015; Noctor et al., 2004; Tau and Peterson, 2010). Upon treatment with RA, the SH-SY5Y cells differentiate into more mature neuronal phenotypes (Korecka et al., 2013; Kovalevich and Langford, 2013; Påhlman et al., 1984). By exposing SH-SY5Y cells with chemicals during differentiation we can elucidate effects on cellular, molecular and transcriptional levels that affect mechanisms that are important for neuronal development (Attoff et al., 2020). These mechanisms can be studied in a 6-day differentiation protocol requiring only one medium exchange step at day 3 and no addition of growth factors compared to other neuronal *in vitro* models (Kobolak et al., 2020; Pistollato et al., 2020). This study aimed to evaluate the SH-SY5Y cell line for the development of a robust and cost-effective candidate test system to be used for *in vitro* DNT evaluation. Ninety-three mRNA markers for diseases and functions in the nervous system were selected using transcriptomic approaches at concentrations attenuating neurite outgrowth, but with no or minimal effect on cell viability. In this study, an automated live cell imaging protocol has successfully been developed using Hoechst-33342 and calcein-AM staining. The protocol presents a time and cost-effective way to measure neurite outgrowth avoiding fixation of cells and staining with primary and secondary antibodies.

Rotenone is a mitochondrial complex I inhibitor pesticide, known to cause neurodegeneration and parkinsonian-like symptoms (Saravanan et al., 2005). In addition, other studies have shown that rotenone also affects the developing brain by inhibiting neuronal differentiation and migration (Pamies et al., 2018; Schmitz et al., 2021). In this study, rotenone attenuated neurite outgrowth at 2 orders of magnitude lower concentration than the concentration affecting cell viability. This specific effect of rotenone on neurites has been observed previously in differentiating dopaminergic LUHMES cells, in differentiated SH-SY5Y cells (Delp et al., 2021) and in differentiated NT2 neuronal precursor cells (Schmitz et al., 2021). Other studies have shown that rotenone is more toxic to developing neurons compared to mature neurons (Krug et al., 2013; Pamies et al., 2018). Taken together, these results support our findings from the differentiating SH-SY5Y neuroblasts that neurite outgrowth is a very sensitive endpoint during rotenone exposure, which may be attributed to its dopaminergic phenotype (Delp et al., 2021; Kovalevich and Langford, 2013; Lopes et al., 2010). In this study, gene expression analysis was performed on SH-SY5Y cells that were exposed to 7.3 nM of rotenone, i.e. estimated EC_{20} for neurite outgrowth, during differentiation. The exposure of rotenone resulted in 32 DEGs ($p < 0.05$) out of the 93 genes studied, indicating that rotenone affected expression of the most genes compared with the other compounds studied. Several of the DEGs affected by rotenone are linked to proteins that are associated to intracellular calcium homeostasis (*ENDRA, CHRM2, S1PR3, RYR1, CDH23, CHRNA7, CHRM1, NRXN1, CACNA1E*) and neurite outgrowth (*SEMA4A, EFNB2, DPYSL3, TUBA4A*). In agreement to this, RNA-seq performed on 2, 4 and 8 weeks differentiated iPSC-derived "brain" spheres after 24 h of rotenone exposure showed a down-regulation of the "Calcium Reabsorption pathway" at all 3 timepoints (Pamies et al., 2018).

Valproic acid is a pharmaceutical drug, primarily used to treat epilepsy, migraine and bipolar disorder. However, it is classified as a potent teratogen and causes DNT. Prenatal exposure to VPA is associated with an increased risk of ASD compared to children of mothers who did not use VPA (Christensen et al., 2013; Rasalam et al., 2005; Taleb et al., 2021). In addition, VPA causes transcriptomic alterations by inhibiting histone deacetylase (Phiel et al., 2001). In our study, VPA attenuated neurite outgrowth in a concentration dependent manner, but the cell viability was also affected at only slightly higher concentrations. Previous findings have observed contradicting results regarding the effect on neurite outgrowth during VPA exposure, where it has been either inhibited or enhanced. The variances in response to VPA in different test

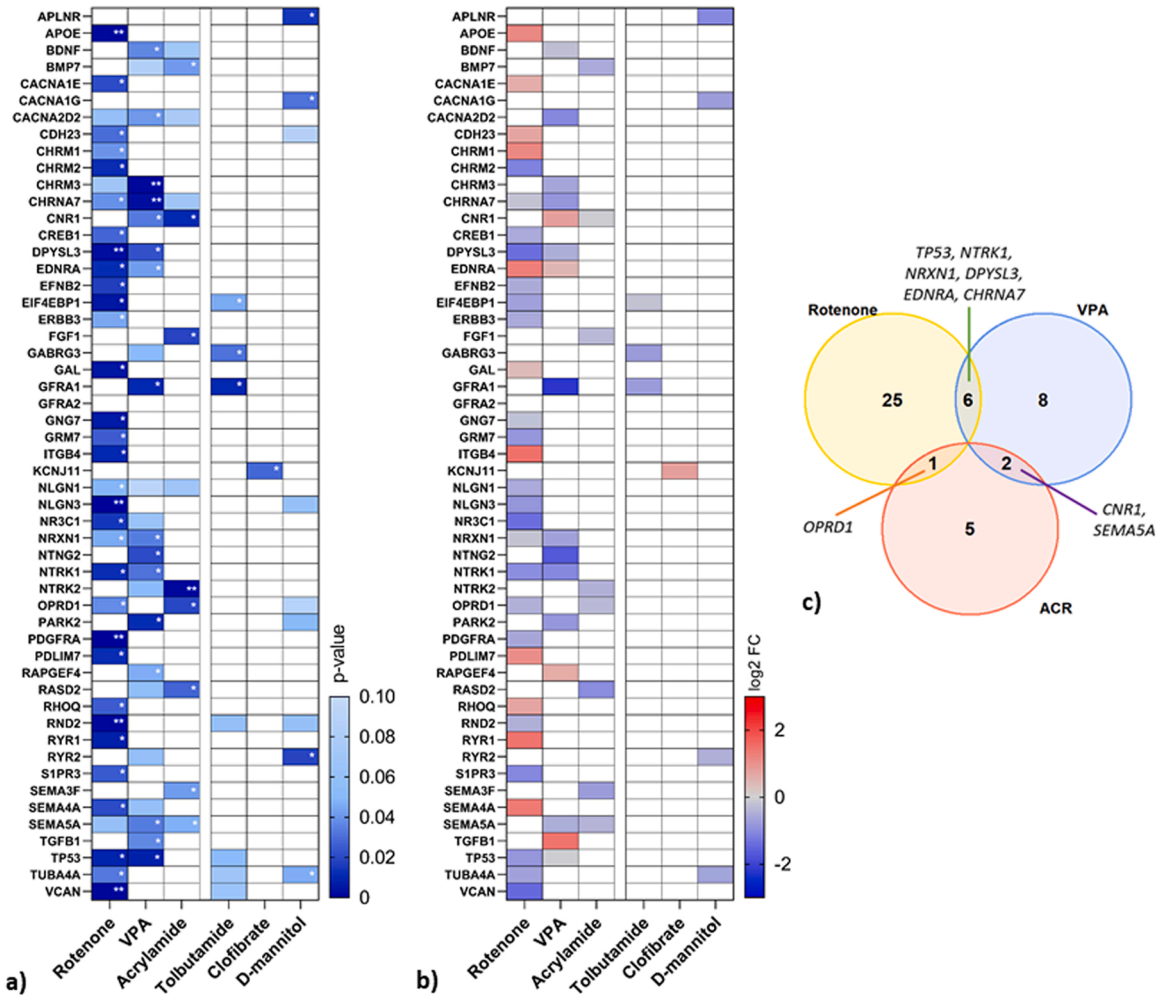

Fig. 6. The effect of rotenone, valproic acid (VPA), acrylamide, tolbutamide, clofibrate and D-mannitol on gene expression in SH-SY5Y cells during differentiation. RT-qPCR analysis of 93 markers after 6 days of exposure to non-cytotoxic concentrations. The 53 genes presented here were differentially expressed by one or more compounds. The results of 3–4 biological replicates were analyzed using a paired parametric multiple t-test, *$p \leq 0.05$, **$p \leq 0.005$. The heat map intensity in a) displays results with $p < 0.1$, illustrating that some genes were close to be statistically differentially expressed by all DNT compounds. The heatmap intensity in b) displays the log2 FC expression of the significantly dysregulated genes ($p < 0.05$). c) Venn diagram illustrating the overlap in differentially expressed genes ($p < 0.05$) between rotenone, ACR and VPA.

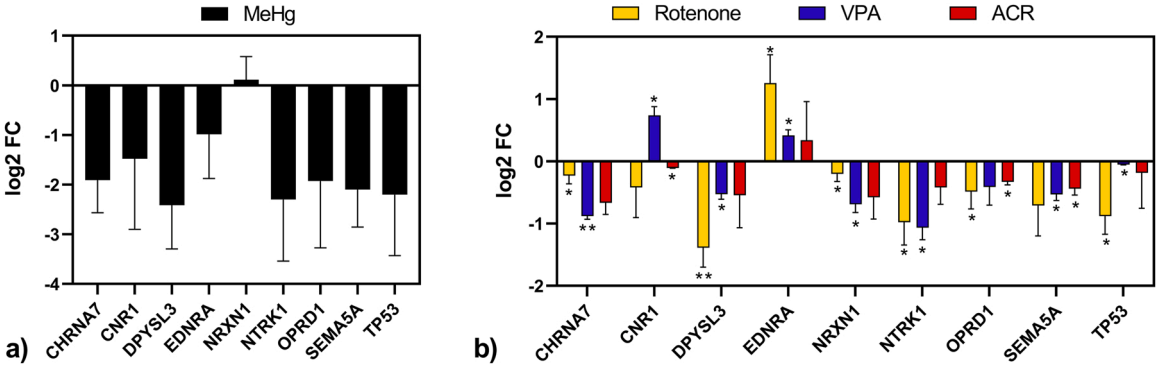

Fig. 7. Validation of the DEGs in common by MeHg. a) RT-qPCR analysis by mono-primers of 9 DEGs after exposing SH-SY5Y cells for 6 days with 0.8 nM MeHg during differentiation. The data are presented as the mean of the log2 FC expression of 2 biological replicates ($n = 2$). b) RT-qPCR analysis from 384-well pre-casted primePCR plates of the 9 DEGs in common after exposure to rotenone, VPA and ACR. The data are presented as the mean ± SD of the log2 FC expression of 3–4 biological replicates. The results of 2–4 biological replicates were analyzed using a paired parametric multiple t-test, *$p \leq 0.05$, **$p \leq 0.005$.

systems might be related to epigenetic modifications in terms of attenuated deacetylation (Phiel et al., 2001; Shafique and Winn, 2021). Six days of exposure to 75 μM VPA during differentiation significantly dysregulated 16 genes in SH-SY5Y cells, including downregulation of *BDNF* expression. Brain-derived neurotrophic factor has been suggested as a key event (KE) for DNT in the adverse outcome pathway (AOP) ID

13 (www.aopwiki.org/aops/13) by Sachana and coworkers (Sachana et al., 2018) and was a centrally located KE in the AOP network for neurotoxicity developed by Spînu et al. (Spînu et al., 2022). In addition, VPA downregulated *TP53*, which can be explained by the fact that VPA inhibits HDACs that interacts with several transcription factors. In 2015, Paradis and Hales showed that VPA exposure of murine limb cultures resulted in a concentration dependent increase of p53 acetylation (Paradis and Hales, 2015). Furthermore, VPA also downregulated genes that are involved in axonal outgrowth (*NTNG2, NRXN1* and *SEMA5A*). Meganathan et al. showed that *NTNG2* (encoding Nerin G2) and *NRXN1* (encoding Neurexin 1) were upregulated in human embryonic stem cell (hESC) exposed to 2 mM VPA during 14 days of differentiation (Meganathan et al., 2015). Similarly, upregulation of *NRXN1* and downregulation of *SEMA5A* was observed in an early neurogenesis hESC model exposed to 1.2 mM VPA during 10 days of differentiation (Krug et al., 2013). The fact that *NTNG2* and *NRXN1* were upregulated, compared to the downregulation seen in differentiating SH-SY5Y cells, might be explained by differences in concentrations and test systems as discussed above for effects of VPA on DNT endpoints.

Acrylamide is a known neurotoxic compound formed in food stuff during heat treatment as a result of the Maillard reaction (Mottram et al., 2002; Stadler et al., 2002). Acrylamide reaches the fetus via placental transfer and has also been detected in breast milk (Sörgel et al., 2002; Von Stedingk et al., 2011). *In vitro* studies have shown that ACR attenuates neuronal differentiation, sustains proliferation and alters expression of genes in the RA and CREB signaling pathways (Attoff et al., 2016; Attoff et al., 2020). In our previous study, ACR decreased neurite outgrowth after exposure during 3 and 6 days of differentiation in SH-SY5Y cells that were exposed to concentrations 10,0000 times lower than the lowest cytotoxic concentration (Attoff et al., 2016). In agreement with this, previous findings have observed that non-cytotoxic concentrations of ACR inhibited neurite outgrowth and neural network formation during differentiation (de Leeuw et al., 2022; Frimat et al., 2010). Thus, the specific effect of ACR on neurite outgrowth in differentiating neuronal cultures is robust and the concentration selected for gene expression analysis in the present study was based on previous findings (Attoff et al., 2016, 2020). Eight genes (*NTRK2;* Neurotrophic Receptor Tyrosine Kinase 2, receptor of BDNF*; CNR1, FGF1, OPRD1, RASD2, BMP7, SEMA3F* and *SEMA5A;* Semaphorin 3 F and 5A, respectively) were significantly dysregulated after exposure to 70 μM ACR during 6 days of differentiation. Surprisingly, *BDNF* expression was not statistically significantly downregulated, as earlier observed in SH-SY5Y cells after 9 days of exposure during differentiation at both mRNA and protein levels of BDNF (Attoff et al., 2020). The reason may be the shorter duration of exposure (6 days instead of 9 days) and one less repeated dosing, or simply that only 3 biological replicates were analyzed, giving less statistical power. Still, the p-value was 0.07, i.e. close to being statistically significant at the 95% level. The downregulation of *NTRK2* also agrees with our previous finding in SH-SY5Y cells exposed to 70 μM ACR during 9 days of differentiation (Attoff et al., 2020). Hence, the SH-SY5Y cell model is not only robust and well characterized in terms of neurite outgrowth, it also provides reproducible transcriptomic results after exposure during differentiation. The fact that it was shown in several studies that ACR attenuates BDNF signaling and can be classified as a DNT inducing compound with high probability, is further supported in a recently published quantitative AOP model (Spînu et al., 2022).

Accidental exposure to environmental MeHg has been associated with severe neurotoxic effects in the developing brain (Aaseth et al., 2020; Grandjean et al., 1997). Prenatal exposure to MeHg causes neural tube defects and mental retardation (Grandjean and Herz, 2011). However, the specific mode of action remains unclear, but interference with thiol moieties in proteins is the most accepted mechanism for neurotoxicity (Rabenstein et al., 1982). Despite the unknown primary or most sensitive target, MeHg has been widely used as a positive control compound for DNT studies, including neurite outgrowth inhibition (Attoff et al., 2017; Krug et al., 2013; Stiegler et al., 2011). Similar to VPA, MeHg attenuated neurite outgrowth in the same concentration dependent pattern as cell viability, which agrees with previous findings (Stiegler et al., 2011). Because of the strong association with adverse neurodevelopment, we used MeHg for validation of the 9 DEGs that were commonly dysregulated by ACR, rotenone and VPA.

Our hypothesis was that compounds that cause DNT should affect expression of genes that are involved in annotations for neuronal function and disease, and were significantly involved during differentiation of the SH-SY5Y cells, in a similar pattern. However, there was no common overlap in DEGs between rotenone, VPA and ACR at $p < 0.05$. Yet, there were 6 DEGs in common between VPA and rotenone (*TP53, NTRK1, NRXN1 DPYSL3, EDNRA, CHRNA7*), 1 DEG in common between ACR and rotenone (*OPRD1*) and 2 DEGs in common between VPA and ACR (*CNR1* and *SEMA5A*). These 9 genes were studied by exposing SH-SY5Y cells during 6 days of differentiation to 0.8 nM, i.e. a concentration of MeHg that corresponded to the approximately highest non-cytotoxic concentration in this study. For comparison, this concentration is about 10 times lower than 2–8.5 μg/L that has been detected in human umbilical cord blood (Lozano et al., 2022). Comparing the log2 FC expression between the 9 genes after exposure to MeHg in 2 independent experiments in a different qPCR set-up, we can see that most genes follow the same dysregulation pattern as after exposure to rotenone, VPA and ACR except for *EDNRA* and *NRXN1* that were downregulated and upregulated by MeHg, respectively, whilst being up- and downregulated, respectively, by the other compounds. Similarly, *CNR1* was downregulated by MeHg, rotenone and ACR whilst being upregulated by VPA.

Rotenone, VPA, ACR and MeHg are all classified as known DNTs, but they are neither chemically related, nor sharing known similar molecular mode(s) of action. It is therefore logical that they regulate different developmental mechanisms and signaling pathways, which can explain the variance in gene expression and lack of overlap in DEGs. Nevertheless, expression of *SEMA5A* was significantly downregulated by both ACR and VPA and the same expression pattern was seen for rotenone ($p = 0.06$) and MeHg. In this regard, *SEMA5A* is a member of the semaphorin family, which encodes membrane proteins with a semaphorin domain. Semaphorins play an important role in axonal guidance and synaptogenesis during neuronal development where it has been shown to act both as an attractor and repellant for neurite outgrowth, depending on which receptor it interacts with (Van Battum et al., 2015; Sadanandam et al., 2010). In addition, *SEMA5A* has previously been suggested as a susceptibility gene for ASD where mRNA downregulation has been detected in B lymphocytes microdeletions in patients diagnosed with ASD (Melin et al., 2006; Mosca-Boidron et al., 2015; Weiss et al., 2009). It is generally hypothesized that ASD is caused by increased connectivity between specific brain regions in combination with decreased connectivity within other brain regions (Delmonte et al., 2013; McFadden and Minshew, 2013; Xu et al., 2019). Increased connectivity would lead to increased spine density whilst reduced connectivity between regions are believed to appear due to deficient axonal outgrowth, which might be caused by impaired SEMA5A-cued axonal guidance (Hutsler and Zhang, 2010; Poelmans et al., 2013). Yet, there is still a lack of evidence in linking the findings on *SEMA5A* function to DNT.

The expression of *CHRNA7,* encoding the α7 subunit of nAChR, was significantly downregulated by both rotenone and VPA. The same expression pattern was seen for ACR ($p = 0.068$) and MeHg, suggesting that *CHRNA7* may be another candidate marker for DNT. In this regard, *CHRNA7* is widely expressed in both the peripheral and central nervous system and has genetically been linked to multiple neuronal disorders such as schizophrenia, autism, and ADHD (Stephens et al., 2009; Williams et al., 2012). In the brain, α7nAChRs are found both presynaptically in GABAergic and glutamatergic neurons (Bürli et al., 2010; Cheng and Yakel, 2014). Activation of nAChR leads to positive modulation of NMDA receptor-dependent synaptic plasticity (Yang et al., 2013). Thus,

a downregulation of *CHRNA7* expression might lead to loss of synaptic plasticity.

The negative control compounds tolbutamide and clofibrate did neither cause any significant effect on neurite outgrowth, nor cell viability at the tested concentrations. D-mannitol induced cytotoxicity after exposure to 100 and 500 mM but did not affect neurite outgrowth. As a pharmacologically and metabolically inert compound (Turina et al., 2008), D-mannitol is used clinically as a diuretic drug to relieve edema by osmosis. Administration of D-mannitol can cause hyperosmolarity which can lead to impaired cellular metabolism (Grauso et al., 2019; Mao et al., 2008). Considering the inertness of D-mannitol and that 2x the final concentrations were added at the repeated exposure, the final concentration might have been slightly higher on day 3–6, than indicated in our experiments. This might explain why cell viability was decreased at the high concentrations since resazurin assay measured metabolic activity. In addition, the therapeutic concentrations in plasma has been reported in a range between 1 and 41 mM i.e. approximately 100 times lower than the highest concentrations tested here (Norlén et al., 2009). Nevertheless, D-mannitol has previously been successfully used as a negative control compound for DNT in NPC test systems and is listed as a negative model compound for DNT (Aschner et al., 2017; Attoff et al., 2017; Krug et al., 2013; Martin et al., 2022). Despite being considered as negative control compounds, D-mannitol dysregulated 4 genes (*APLNR, CACNA1G, RYR2* and *TUBA4A*), clofibrate 1 gene (*KCNJ11*) and tolbutamide 3 genes (*EIF4EBP1, GABRG3* and *GFRA1*) after exposure for 6 days during differentiation. From them, *EIF4EBP1* (encoding a translation repressor protein) and *TUBA4A* (encoding an α-tubulin protein in microtubule) were also dysregulated by rotenone and *GFRA1* (encoding the receptor for glial cell line-derived neurotrophic factor) by VPA. Otherwise, no overlapping DEGs with the positive DNT compounds were observed. Importantly, none of the negative control compounds affected the expression of the 2 biomarker candidates *SEMA5A* and *CHRNA7* found in the study, nor the DNT biomarker *BDNF* or its receptor *NTRK2*. The choice of negative control compounds for DNT studies *in vitro* is difficult because the lack of placental and blood-brain barriers. However, out of the 3 negative control compounds selected in this study, clofibrate can be considered the most suitable for the SH-SY5Y cells.

Applying a transcriptomics approach, in combination with functional data has been done previously, with the aim to identify biomarkers that can be used for DNT assessment *in vitro*. Krug et al. evaluated 5 hESC systems mirroring different phases of neuronal development, as alternative NAMs for DNT and reproductive toxicity. Not only did the test systems differ in their transcriptomic responses, but VPA and MeHg displayed different gene expression changes with little overlap (Krug et al., 2013). Recently, de Leeuw et al. (2022) presented a test system where human NPCs differentiate during 10 days into a neuron-astrocyte co-culture. Following exposure to ACR, VPA, chlorpyrifos, fluoxetine or MeHg transcriptomic analysis revealed that each compound dysregulated gene ontology terms in a unique combination. Similar to our findings, overlap in DEGs were found between a subset of the compounds but no overlap in DEGs were observed between all (de Leeuw et al., 2022).

5. Conclusions

The different effects of rotenone, VPA, ACR and MeHg on neurite outgrowth and gene expression further indicate that DNT is mediated by more than one mechanism. The developmental stage of the test system, timing and the duration of exposure may also affect the DNT outcome. No list of "fingerprint" mRNA biomarkers for future DNT screening was obtained among the 93 markers studied, which could be explained by the differences in mechanisms of toxicity between the positive DNT chemicals. However, *SEMA5A* and *CHRNA7* were identified as promising biomarkers because they were dysregulated by all 4 positive DNT compounds, they have documented connection to developmental disorders and the expression was not altered by any of the negative control compounds. Hence, *SEMA5A* and *CHRNA7* should be further investigated as DNT biomarkers and may also be considered in future DNT AOP frameworks.

Finances

This study was supported by the Swedish Fund for Research without Animal Experiments (grants N2018-0004, F2019-0009, F2020-0006) and the Swedish Research Council (grant 2018-03269).

CRediT authorship contribution statement

MGH: Data curation, Formal analysis, Investigation, Methodology, Software, Validation, Visualization, Writing – review & editing. **YJ:** Data curation, Formal analysis, Investigation, Methodology, Software, Validation, Visualization, Writing – original draft, Writing – review & editing. **ACU:** Conceptualization, Data curation, Formal analysis, Investigation, Methodology, Writing – review & editing. **EI:** Data curation, Formal analysis, Investigation, Methodology, Software, Validation. **NG:** Data curation, Writing – review & editing. **AG:** Conceptualization, Formal analysis, Software, Validation, Writing – review & editing. **AF:** Conceptualization, Funding acquisition, Project administration, Resources, Supervision, Visualization, Writing – review & editing.

Declaration of Competing Interest

The authors declare that they have no known competing financial interests or personal relationships that could have appeared to influence the work reported in this paper.

Data Availability

A link has been shared in the manuscript.

Acknowledgements

We thank Chris Molenaar at the Imaging Facility at Stockholm University (IFSU) for valuable support during the development of the live-cell imaging methodology.

Appendix A. Supporting information

Supplementary data associated with this article can be found in the online version at doi:10.1016/j.neuro.2023.05.011.

References

Aaseth, J., Wallace, D.R., Vejrup, K., Alexander, J., 2020. Methylmercury and developmental neurotoxicity: A global concern. Curr. Opin. Toxicol. 19, 80–87. https://doi.org/10.1016/J.COTOX.2020.01.005.

Aschner, M., Ceccatelli, S., Daneshian, M., Fritsche, E., Hasiwa, N., Hartung, T., Hogberg, H.T., Leist, M., Li, A., Mundy, W.R., Padilla, S., Piersma, A.H., Bal-Price, A., Seiler, A., Westerink, R.H., Zimmer, B., Lein, P.J., 2017. Reference compounds for alternative test methods to indicate developmental neurotoxicity (DNT) potential of chemicals: Example lists and criteria for their selection and use. ALTEX - Altern. Anim. Exp. 34, 49–74. https://doi.org/10.14573/ALTEX.1604201.

Attoff, K., Kertika, D., Lundqvist, J., Oredsson, S., Forsby, A., 2016. Acrylamide affects proliferation and differentiation of the neural progenitor cell line C17.2 and the neuroblastoma cell line SH-SY5Y. Toxicol. In Vitro 35, 100–111. https://doi.org/10.1016/J.TIV.2016.05.014.

Attoff, K., Gliga, A., Lundqvist, J., Norinder, U., Forsby, A., 2017. Whole genome microarray analysis of neural progenitor C17.2 cells during differentiation and validation of 30 neural mRNA biomarkers for estimation of developmental neurotoxicity. PLoS One 12, e0190066. https://doi.org/10.1371/JOURNAL.PONE.0190066.

Attoff, K., Johansson, Y., Cediel-Ulloa, A., Lundqvist, J., Gupta, R., Caiment, F., Gliga, A., Forsby, A., 2020. Acrylamide alters CREB and retinoic acid signalling pathways during differentiation of the human neuroblastoma SH-SY5Y cell line. Sci. Rep. 1 (10), 1–15. https://doi.org/10.1038/s41598-020-73698-6.

Bacchelli, E., Battaglia, A., Cameli, C., Lomartire, S., Tancredi, R., Thomson, S., Sutcliffe, J.S., Maestrini, E., 2015. Analysis of CHRNA7 rare variants in autism spectrum disorder susceptibility. Am. J. Med. Genet. Part A 167, 715–723. https://doi.org/10.1002/AJMG.A.36847.

Bal-Price, A., Hogberg, H.T., Crofton, K.M., Daneshian, M., FitzGerald, R.E., Fritsche, E., Heinonen, T., Hougaard Bennekou, S., Klima, S., Piersma, A.H., Sachana, M., Shafer, T.J., Terron, A., Monnet-Tschudi, F., Viviani, B., Waldmann, T., Westerink, R. H.S., Wilks, M.F., Witters, H., Zurich, M.G., Leist, M., 2018a. Recommendation on test readiness criteria for new approach methods in toxicology: exemplified for developmental neurotoxicity. ALTEX - Altern. Anim. Exp. 35, 306–352. https://doi.org/10.14573/ALTEX.1712081.

Bal-Price, A., Pistollato, F., Sachana, M., Bopp, S.K., Munn, S., Worth, A., 2018b. Strategies to improve the regulatory assessment of developmental neurotoxicity (DNT) using in vitro methods. Toxicol. Appl. Pharmacol. 354, 7–18. https://doi.org/10.1016/J.TAAP.2018.02.008.

Bandeira, C.E., Grevet, E.H., Cupertino, R.B., Tavares, M.E. d A., Gusmão, C.S., Kappel, D.B., Vitola, E.S., Picon, F.A., Rohde, L.A., da Silva, B.S., Bau, C.H.D., Rovaris, D.L., 2021. The role of glucocorticoid receptor gene in the association between attention deficit-hyperactivity disorder and smaller brain structures. J. Neural Transm. 128, 1907–1916. https://doi.org/10.1007/S00702-021-02425-W.

Boyle, C.A., Boulet, S., Schieve, L.A., Cohen, R.A., Blumberg, S.J., Yeargin-Allsopp, M., Visser, S., Kogan, M.D., 2011. Trends in the prevalence of developmental disabilities in US children, 1997-2008. Pediatrics 127, 1034–1042. https://doi.org/10.1542/peds.2010-2989.

Budday, S., Steinmann, P., Kuhl, E., 2015. Physical biology of human brain development. Front. Cell. Neurosci. 9, 257. https://doi.org/10.3389/FNCEL.2015.00257.

Bürli, T., Baer, K., Ewers, H., Sidler, C., Fuhrer, C., Fritschy, J.M., 2010. Single particle tracking of α7 nicotinic AChR in hippocampal neurons reveals regulated confinement at glutamatergic and GABAergic perisynaptic sites. PLoS One 5, e11507. https://doi.org/10.1371/JOURNAL.PONE.0011507.

Carrillo-García, C., Prochnow, S., Simeonova, I.K., Strelau, J., Hölzl-Wenig, G., Mandl, C., Unsicker, K., von Bohlen, Halbach, O., Ciccolini, F., 2014. Growth/differentiation factor 15 promotes EGFR signalling, and regulates proliferation and migration in the hippocampus of neonatal and young adult mice. Development 141, 773–783. https://doi.org/10.1242/DEV.096131.

Cheng, Q., Yakel, J.L., 2014. Presynaptic α7 nicotinic acetylcholine receptors enhance hippocampal mossy fiber glutamatergic transmission via PKA activation. J. Neurosci. 34, 124. https://doi.org/10.1523/JNEUROSCI.2973-13.2014.

Christensen, J., Grnøborg, T.K., Sørensen, M.J., Schendel, D., Parner, E.T., Pedersen, L.H., Vestergaard, M., 2013. Prenatal valproate exposure and risk of autism spectrum disorders and childhood autism. JAMA 309, 1696–1703. https://doi.org/10.1001/JAMA.2013.2270.

Council, N.R., 2000. Scientific frontiers in developmental toxicology and risk assessment. Scientific Frontiers in Developmental Toxicology and Risk Assessment. National Academies Press. https://doi.org/10.17226/9871.

Crofton, K., Fritsche, E., Ylikomi, T., Bal-Price, A., 2014. International STakeholder NETwork (ISTNET) for creating a developmental neurotoxicity testing (DNT) roadmap for regulatory purposes. ALTEX - Altern. Anim. Exp. 31, 223–224. https://doi.org/10.14573/ALTEX.1402121.

Delmonte, S., Gallagher, L., O'Hanlon, E., McGrath, J., Balsters, J.H., 2013. Functional and structural connectivity of frontostriatal circuitry in autism spectrum disorder. Front. Hum. Neurosci. 0, 430. https://doi.org/10.3389/FNHUM.2013.00430.

Delp, J., Cediel-Ulloa, A., Suciu, I., Kranaster, P., van Vugt-Lussenburg, B.M., Munic Kos, V., van der Stel, W., Carta, G., Bennekou, S.H., Jennings, P., van de Water, B., Forsby, A., Leist, M., 2021. Neurotoxicity and underlying cellular changes of 21 mitochondrial respiratory chain inhibitors. Arch. Toxicol. 95, 591–615. https://doi.org/10.1007/S00204-020-02970-5.

ECHA, 2018. REACH registration results [WWW Document]. URL ⟨https://echa.europa.eu/sv/reach-registrations-since-2008⟩ (accessed 11.16.22).

EPA, 1998. USEPA OPPTS 870.6300, Developmental Neurotoxicity Study [WWW Document]. EPA Office of Chemical Safety and Polution Prevention. Washington, U. S. URL ⟨https://nepis.epa.gov/Exe/ZyPURL.cgi?Dockey=P100IRWO.txt⟩ (accessed 7.1.21).

EPA, 2022. Toxic Substances Control Act Chemical Substance Inventory [WWW Document]. URL ⟨https://www.epa.gov/tsca-inventory/how-access-tsca-inventory⟩ (accessed 11.16.22).

Fathe, K., Palacios, A., Finnell, R.H., 2014. Novel mechanism for valproate-induced teratogenicity. Birth Defects Res. Part A Clin. Mol. Teratol. 100, 592. https://doi.org/10.1002/BDRA.23277.

Fennell, T.R., Friedman, M.A., 2005. Comparison of acrylamide metabolism in humans and rodents. Adv. Exp. Med. Biol. 561, 109–116. https://doi.org/10.1007/0-387-24980-X_9.

Frimat, J.P., Sisnaiske, J., Subbiah, S., Menne, H., Godoy, P., Lampen, P., Leist, M., Franzke, J., Hengstler, J.G., Van Thriel, C., West, J., 2010. The network formation assay: a spatially standardized neurite outgrowth analytical display for neurotoxicity screening. Lab Chip 10, 701–709. https://doi.org/10.1039/B922193J.

Fritsche, E., Crofton, K.M., Hernandez, A.F., Bennekou, S.H., Leist, M., Bal-Price, A., Reaves, E., Wilks, M.F., Terron, A., Solecki, R., Sachana, M., Gourmelon, A., 2017. OECD/EFSA workshop on developmental neurotoxicity (DNT): The use of non-animal test methods for regulatory purposes. ALTEX - Altern. Anim. Exp. 34, 311–315. https://doi.org/10.14573/ALTEX.1701171.

Fritsche, E., Barenys, M., Klose, J., Masjosthusmann, S., Nimtz, L., Schmuck, M., Wuttke, S., Tigges, J., 2018a. Current availability of stem cell-based in vitro methods for developmental neurotoxicity (DNT) testing. Toxicol. Sci. 165, 21–30. https://doi.org/10.1093/TOXSCI/KFY178.

Fritsche, E., Barenys, M., Klose, J., Masjosthusmann, S., Nimtz, L., Schmuck, M., Wuttke, S., Tigges, J., 2018b. Development of the concept for stem cell-based developmental neurotoxicity evaluation. Toxicol. Sci. 165, 14–20. https://doi.org/10.1093/TOXSCI/KFY175.

Fritsche, E., Alm, H., Baumann, J., Geerts, L., Håkansson, H., Masjosthusmann, S., Witters, H., 2015. Literature review on in vitro and alternative Developmental Neurotoxicity (DNT) testing methods. EFSA Supporting Publications 12, 778E. https://doi.org/10.2903/SP.EFSA.2015.EN-778.

Galasko, G.T., 2017. Insulin, oral hypoglycemics, and glucagon (Seventh Edition). Pharmacol. Ther. Dent. 437–445. https://doi.org/10.1016/B978-0-323-39307-2.00031-X.

Grandjean, P., Herz, K.T., 2011. Methylmercury and brain development: imprecision and underestimation of developmental neurotoxicity in humans. Mt. Sinai J. Med. 78, 107–118. https://doi.org/10.1002/MSJ.20228.

Grandjean, P., Landrigan, P.J., 2006. Developmental neurotoxicity of industrial chemicals. Lancet 368, 2167–2178.

Grandjean, P., Weihe, P., White, R.F., Debes, F., Araki, S., Yokoyama, K., Murata, K., SØrensen, N., Dahl, R., JØrgensen, P.J., 1997. Cognitive deficit in 7-year-old children with prenatal exposure to methylmercury. Neurotoxicol. Teratol. 19, 417–428. https://doi.org/10.1016/S0892-0362(97)00097-4.

Grauso, M., Lan, A., Andriamihaja, M., Bouillaud, F., Blachier, F., 2019. Hyperosmolar environment and intestinal epithelial cells: impact on mitochondrial oxygen consumption, proliferation, and barrier function in vitro. Sci. Rep. 9. https://doi.org/10.1038/S41598-019-47851-9.

Hogberg, H.T., Kinsner-Ovaskainen, A., Coecke, S., Hartung, T., Bal-Price, A.K., 2010. mRNA expression is a relevant tool to identify developmental neurotoxicants using an in vitro approach. Toxicol. Sci. 113, 95–115. https://doi.org/10.1093/toxsci/kfp175.

Hutsler, J.J., Zhang, H., 2010. Increased dendritic spine densities on cortical projection neurons in autism spectrum disorders. Brain Res. 1309, 83–94. https://doi.org/10.1016/J.BRAINRES.2009.09.120.

Jiang, W.-W., Zhang, Z.-Z., He, P.-P., Jiang, L.-P., Chen, J.-Z., Zhang, X.-T., Hu, M., Zhang, Y.-K., Ouyang, X.-P., 2021. Emerging roles of growth differentiation factor-15 in brain disorders (Review). Exp. Ther. Med. 22, 1–11. https://doi.org/10.3892/ETM.2021.10705.

Kobolak, J., Teglasi, A., Bellak, T., Janstova, Z., Molnar, K., Zana, M., Bock, I., Laszlo, L., Dinnyes, A., 2020. Human induced pluripotent stem cell-derived 3D-neurospheres are suitable for neurotoxicity screening. Cells 9. https://doi.org/10.3390/CELLS9051122.

Koch, K., Bartmann, K., Hartmann, J., Kapr, J., Klose, J., Kuchovská, E., Pahl, M., Schlüppmann, K., Zühr, E., Fritsche, E., 2022. Scientific validation of human neurosphere assays for developmental neurotoxicity evaluation. Front. Toxicol. 4. https://doi.org/10.3389/FTOX.2022.816370.

Korecka, J.A., van Kesteren, R.E., Blaas, E., Spitzer, S.O., Kamstra, J.H., Smit, A.B., Swaab, D.F., Verhaagen, J., Bossers, K., 2013. Phenotypic characterization of retinoic acid differentiated SH-SY5Y cells by transcriptional profiling. PLoS One 8, e63862. https://doi.org/10.1371/JOURNAL.PONE.0063862.

Kovalevich, J., Langford, D., 2013. Considerations for the use of SH-SY5Y neuroblastoma cells in neurobiology. Methods Mol. Biol. 1078, 9–21. https://doi.org/10.1007/978-1-62703-640-5_2.

Krämer, A., Green, J., Pollard, J., Tugendreich, S., 2014. Causal analysis approaches in ingenuity pathway analysis. Bioinformatics 30, 523–530. https://doi.org/10.1093/BIOINFORMATICS/BTT703.

Krebs, A., van Vugt-Lussenburg, B.M.A., Waldmann, T., Albrecht, W., Boei, J., ter Braak, B., Brajnik, M., Braunbeck, T., Brecklinghaus, T., Busquet, F., Dinnyes, A., Dokler, J., Dolde, X., Exner, T.E., Fisher, C., Fluri, D., Forsby, A., Hengstler, J.G., Holzer, A.K., Janstova, Z., Jennings, P., Kisitu, J., Kobolak, J., Kumar, M., Limonciel, A., Lundqvist, J., Mihalik, B., Moritz, W., Pallocca, G., Ulloa, A.P.C., Pastor, M., Rovida, C., Sarkans, U., Schimming, J.P., Schmidt, B.Z., Stöber, R., Strassfeld, T., van de Water, B., Wilmes, A., van der Burg, B., Verfaillie, C.M., von Hellfeld, R., Vrieling, H., Vrijenhoek, N.G., Leist, M., 2020. The EU-ToxRisk method documentation, data processing and chemical testing pipeline for the regulatory use of new approach methods. Arch. Toxicol. 7 (94), 2435–2461. https://doi.org/10.1007/S00204-020-02802-6.

Krug, A.K., Kolde, R., Gaspar, J.A., Rempel, E., Balmer, N.V., Meganathan, K., Vojnits, K., Baquié, M., Waldmann, T., Ensenat-Waser, R., Jagtap, S., Evans, R.M., Julien, S., Peterson, H., Zagoura, D., Kadereit, S., Gerhard, D., Sotiriadou, I., Heke, M., Natarajan, K., Henry, M., Winkler, J., Marchan, R., Stoppini, L., Bosgra, S., Westerhout, J., Verwei, M., Vilo, J., Kortenkamp, A., Hescheler, J., Hothorn, L., Bremer, S., Van Thriel, C., Krause, K.H., Hengstler, J.G., Rahnenführer, J., Leist, M., Sachinidis, A., 2013. Human embryonic stem cell-derived test systems for developmental neurotoxicity: a transcriptomics approach. Arch. Toxicol. 87, 123–143. https://doi.org/10.1007/S00204-012-0967-3/FIGURES/10.

Langton, S., Gudas, L.J., 2008. CYP26A1 knockout embryonic stem cells exhibit reduced differentiation and growth arrest in response to retinoic acid. Dev. Biol. 315, 331–354. https://doi.org/10.1016/J.YDBIO.2007.12.021.

de Leeuw, V.C., van Oostrom, C.T.M., Wackers, P.F.K., Pennings, J.L.A., Hodemaekers, H.M., Piersma, A.H., Hessel, E.V.S., 2022. Neuronal differentiation pathways and compound-induced developmental neurotoxicity in the human neural progenitor cell test (hNPT) revealed by RNA-seq. Chemosphere 304, 135298. https://doi.org/10.1016/J.CHEMOSPHERE.2022.135298.

Livak, K.J., Wills, Q.F., Tipping, A.J., Datta, K., Mittal, R., Goldson, A.J., Sexton, D.W., Holmes, C.C., 2013. Methods for qPCR gene expression profiling applied to 1440 lymphoblastoid single cells. Methods 59, 71–79. https://doi.org/10.1016/J.YMETH.2012.10.004.

LoPachin, R.M., Gavin, T., Geohagen, B.C., Das, S., 2007. Neurotoxic mechanisms of electrophilic type-2 alkenes: soft soft interactions described by quantum mechanical parameters. Toxicol. Sci. 98, 561–570. https://doi.org/10.1093/TOXSCI/KFM127.

Lopes, F.M., Schröder, R., Júnior, M.L.C., da, F., Zanotto-Filho, A., Müller, C.B., Pires, A. S., Meurer, R.T., Colpo, G.D., Gelain, D.P., Kapczinski, F., Moreira, J.C.F., Fernandes, M., da, C., Klamt, F., 2010. Comparison between proliferative and neuron-like SH-SY5Y cells as an in vitro model for Parkinson disease studies. Brain Res. 1337, 85–94. https://doi.org/10.1016/J.BRAINRES.2010.03.102.

Lozano, M., Yousefi, P., Broberg, K., Soler-Blasco, R., Miyashita, C., Pesce, G., Kim, W.J., Rahman, M., Bakulski, K.M., Haug, L.S., Ikeda-Araki, A., Huel, G., Park, J., Relton, C., Vrijheid, M., Rifas-Shiman, S., Oken, E., Dou, J.F., Kishi, R., Gutzkow, K. B., Annesi-Maesano, I., Won, S., Hivert, M.F., Fallin, M.D., Vafeiadi, M., Ballester, F., Bustamante, M., Llop, S., 2022. DNA methylation changes associated with prenatal mercury exposure: a meta-analysis of prospective cohort studies from PACE consortium. Environ. Res. 204, 112093 https://doi.org/10.1016/J.ENVRES.2021.112093.

Mao, L., Hard, D., Nolden, T., Koppelstatter, A., Klose, J., Himmelbauer, H., Zabel, C., 2008. Pronounced alterations of cellular metabolism and structure due to hyper- Or hypo-osmosis. J. Proteome Res. 7, 3968–3983. https://doi.org/10.1021/PR800245X/ASSET/IMAGES/LARGE/PR-2008-00245X_0008.JPEG.

Martin, M.M., Baker, N.C., Boyes, W.K., Carstens, K.E., Culbreth, M.E., Gilbert, M.E., Harrill, J.A., Nyffeler, J., Padilla, S., Friedman, K.P., Shafer, T.J., 2022. An expert-driven literature review of "negative" chemicals for developmental neurotoxicity (DNT) in vitro assay evaluation. Neurotoxicol. Teratol. 93, 107117 https://doi.org/10.1016/J.NTT.2022.107117.

Martínez, M.A., Lopez-Torres, B., Rodríguez, J.L., Martínez, M., Maximiliano, J.E., Martínez-Larrañaga, M.R., Anadón, A., Ares, I., 2020. Toxicologic evidence of developmental neurotoxicity of Type II pyrethroids cyfluthrin and alpha-cypermethrin in SH-SY5Y cells. Food Chem. Toxicol. 137, 111173 https://doi.org/10.1016/J.FCT.2020.111173.

Masjosthusmann, S., Blum, J., Bartmann, K., Dolde, X., Holzer, A.-K., Stürzl, L.-C., Keßel, E.H., Förster, N., Dönmez, A., Klose, J., Pahl, M., Waldmann, T., Bendt, F., Kisitu, J., Suciu, I., Hübenthal, U., Mosig, A., Leist, M., Fritsche, E., 2020. Establishment of an a priori protocol for the implementation and interpretation of an in-vitro testing battery for the assessment of developmental neurotoxicity. EFSA Supporting Publications 17, 1938E. https://doi.org/10.2903/SP.EFSA.2020.EN-1938.

McFadden, K., Minshew, N.J., 2013. Evidence for dysregulation of axonal growth and guidance in the etiology of ASD. Front. Hum. Neurosci. 0, 671. https://doi.org/10.3389/FNHUM.2013.00671/BIBTEX.

McGuire, C.B., Snipes, G.J., Norden, J.J., 1988. Light-microscopic immunolocalization of the growth- and plasticity-associated protein GAP-43 in the developing rat brain. Dev. Brain Res. 41, 277–291. https://doi.org/10.1016/0165-3806(88)90189-7.

Meganathan, K., Jagtap, S., Srinivasan, S.P., Wagh, V., Hescheler, J., Hengstler, J., Leist, M., Sachinidis, A., 2015. Neuronal developmental gene and miRNA signatures induced by histone deacetylase inhibitors in human embryonic stem cells. Cell Death Dis. 5 (6) https://doi.org/10.1038/cddis.2015.121.

Melin, M., Carlsson, B., Anckarsater, H., Rastam, M., Betancur, C., Isaksson, A., Gillberg, C., Dahl, N., 2006. Constitutional downregulation of SEMA5A expression in autism. Neuropsychobiology 54, 64–69. https://doi.org/10.1159/000096040.

Methaneethorn, J., 2018. A systematic review of population pharmacokinetics of valproic acid. Br. J. Clin. Pharmacol. 84, 816. https://doi.org/10.1111/BCP.13510.

Morel, F.M.M., Kraepiel, A.M.L., Amyot, M., 1998. The chemical cycle and bioaccumulation of mercury. Annu. Rev. Ecol. Syst. 29, 543–566. https://doi.org/10.1146/ANNUREV.ECOLSYS.29.1.543.

Mosca-Boidron, A.L., Gueneau, L., Huguet, G., Goldenberg, A., Henry, C., Gigot, N., Pallesi-Pocachard, E., Falace, A., Duplomb, L., Thevenon, J., Duffourd, Y., ST-Onge, J., Chambon, P., Rivire, J.B., Thauvin-Robinet, C., Callier, P., Marle, N., Payet, M., Ragon, C., Botros, H.G., Buratti, J., Calderari, S., Dumas, G., Delorme, R., Lagarde, N., Pinoit, J.M., Rosier, A., Masurel-Paulet, A., Cardoso, C., Mugneret, F., Saugier-Veber, P., Campion, D., Faivre, L., Bourgeron, T., 2015. A de novo microdeletion of SEMA5A in a boy with autism spectrum disorder and intellectual disability. Eur. J. Hum. Genet. 6 (24), 838–843. https://doi.org/10.1038/ejhg.2015.211.

Mottram, D.S., Wedzicha, B.L., Dodson, A.T., 2002. Acrylamide is formed in the Maillard reaction. Nature 419, 448–449. https://doi.org/10.1038/419448A.

Myren, M., Mose, T., Mathiesen, L., Knudsen, L.E., 2007. The human placenta–an alternative for studying foetal exposure. Toxicol. In Vitro 21, 1332–1340. https://doi.org/10.1016/J.TIV.2007.05.011.

Noctor, S.C., Martinez-Cerdeño, V., Ivic, L., Kriegstein, A.R., 2004. Cortical neurons arise in symmetric and asymmetric division zones and migrate through specific phases. Nat. Neurosci. 2 (7), 136–144. https://doi.org/10.1038/nn1172.

Norlén, H., Allgén, L.G., Wicksell, B., 2009. Mannitol concentrations in blood plasma in connection with transurethral resection of the prostate using mannitol solution as an irrigating fluid. Scand. J. Urol. Nephrol. 20, 119–126. https://doi.org/10.3109/00365598609040559.

O'Brien, J., Wilson, I., Orton, T., Pognan, F., 2000. Investigation of the Alamar Blue (resazurin) fluorescent dye for the assessment of mammalian cell cytotoxicity. Eur. J. Biochem. 267, 5421–5426. https://doi.org/10.1046/J.1432-1327.2000.01606.X.

OECD, 2007. Test No. 426: Developmental Neurotoxicity Study, OECD Guidelines for the Testing of Chemicals, Section 4. OECD. https://doi.org/10.1787/9789264067394-en.

Påhlman, S., Ruusala, A.I., Abrahamsson, L., Mattsson, M.E.K., Esscher, T., 1984. Retinoic acid-induced differentiation of cultured human neuroblastoma cells: a comparison with phorbolester-induced differentiation. Cell Differ. 14, 135–144. https://doi.org/10.1016/0045-6039(84)90038-1.

Pamies, D., Block, K., Lau, P., Gribaldo, L., Pardo, C.A., Barreras, P., Smirnova, L., Wiersma, D., Zhao, L., Harris, G., Hartung, T., Hogberg, H.T., 2018. Rotenone exerts developmental neurotoxicity in a human brain spheroid model. Toxicol. Appl. Pharmacol. 354, 101–114. https://doi.org/10.1016/J.TAAP.2018.02.003.

Paradis, F.H., Hales, B.F., 2015. Valproic acid induces the hyperacetylation of P53, expression of P53 target genes, and markers of the intrinsic apoptotic pathway in midorganogenesis murine limbs. Birth Defects Res. Part B: Dev. Reprod. Toxicol. 104, 177–183. https://doi.org/10.1002/BDRB.21149.

Phiel, C.J., Zhang, F., Huang, E.Y., Guenther, M.G., Lazar, M.A., Klein, P.S., 2001. Histone deacetylase is a direct target of valproic acid, a potent anticonvulsant, mood stabilizer, and teratogen. J. Biol. Chem. 276, 36734–36741. https://doi.org/10.1074/jbc.M101287200.

Pistollato, F., De Gyves, E.M., Carpi, D., Bopp, S.K., Nunes, C., Worth, A., Bal-Price, A., 2020. Assessment of developmental neurotoxicity induced by chemical mixtures using an adverse outcome pathway concept. Environ. Health. 19, 1–26. https://doi.org/10.1186/S12940-020-00578-X.

Poelmans, G., Franke, B., Pauls, D.L., Glennon, J.C., Buitelaar, J.K., 2013. AKAPs integrate genetic findings for autism spectrum disorders. Transl. Psychiatry 3 (6), e270. https://doi.org/10.1038/tp.2013.48.

Proença, S., Escher, B.I., Fischer, F.C., Fisher, C., Grégoire, S., Hewitt, N.J., Nicol, B., Paini, A., Kramer, N.I., 2021. Effective exposure of chemicals in in vitro cell systems: A review of chemical distribution models. Toxicol. In Vitro. 73, 105133 https://doi.org/10.1016/J.TIV.2021.105133.

Rabenstein, D.L., Isab, A.A., Reid, R.S., 1982. A proton nuclear magnetic resonance study of the binding of methylmercury in human erythrocytes. Biochim. Biophys. Acta 720, 53–64. https://doi.org/10.1016/0167-4889(82)90038-6.

Rasalam, A.D., Hailey, H., Williams, J.H.G., Moore, S.J., Turnpenny, P.D., Lloyd, D.J., Dean, J.C.S., 2005. Characteristics of fetal anticonvulsant syndrome associated autistic disorder. Dev. Med. Child Neurol. 47, 551–555. https://doi.org/10.1017/S0012162205001076.

Rice, D., Barone, S., 2000. Critical periods of vulnerability for the developing nervous system: evidence from humans and animal models. Environ. Health Perspect. 108 (3), 511–533. https://doi.org/10.1289/EHP.00108S3511.

Rozman, K.K., Doull, J., Hayes, W.J., 2010. Dose and Time Determining, and Other Factors Influencing, Toxicity. Hayes' Handbook of Pesticide Toxicology, Third Edition: Volume 1 1, 3–101. https://doi.org/10.1016/B978-0-12-374367-1.00001-X.

Sachana, M., Rolaki, A., Bal-Price, A., 2018. Development of the adverse outcome pathway (AOP): chronic binding of antagonist to N-methyl-D-aspartate receptors (NMDARs) during brain development induces impairment of learning and memory abilities of children. Toxicol. Appl. Pharmacol. 354. https://doi.org/10.1016/j.taap.2018.02.024.

Sachana, M., Shafer, T.J., Terron, A., 2021. Toward a better testing paradigm for developmental neurotoxicity: OECD efforts and regulatory considerations. Biology 10, 86. https://doi.org/10.3390/BIOLOGY10020086.

Sadanandam, A., Rosenbaugh, E.G., Singh, S., Varney, M., Singh, R.K., 2010. Semaphorin 5A promotes angiogenesis by increasing endothelial cell proliferation, migration, and decreasing apoptosis. Microvasc. Res. 79, 1–9. https://doi.org/10.1016/J.MVR.2009.10.005.

Saravanan, K.S., Sindhu, K.M., Mohanakumar, K.P., 2005. Acute intranigral infusion of rotenone in rats causes progressive biochemical lesions in the striatum similar to Parkinson's disease. Brain Res. 1049, 147–155. https://doi.org/10.1016/J.BRAINRES.2005.04.051.

Schmitz, A., Dempewolf, S., Tan, S., Bicker, G., Stern, M., 2021. Developmental neurotoxicity of fipronil and rotenone on a human neuronal in vitro test system. Neurotox. Res. 39, 1189–1202. https://doi.org/10.1007/S12640-021-00364-8.

Schwartz, M.P., Hou, Z., Propson, N.E., Zhang, J., Engstrom, C.J., Costa, V.S., Jiang, P., Nguyen, B.K., Bolin, J.M., Daly, W., Wang, Y., Stewart, R., Page, C.D., Murphy, W.L., Thomson, J.A., 2015. Human pluripotent stem cell-derived neural constructs for predicting neural toxicity. Proc. Natl. Acad. Sci. USA 112, 12516–12521. https://doi.org/10.1073/PNAS.1516645112.

Shafique, S., Winn, L.M., 2021. Gestational valproic acid exposure induces epigenetic modifications in murine decidua. Placenta 107, 31–40. https://doi.org/10.1016/J.PLACENTA.2021.03.004.

Smirnova, L., Hogberg, H.T., Leist, M., Hartung, T., 2014. Developmental neurotoxicity – Challenges in the 21st century and in vitro opportunities. ALTEX - Altern. Anim. Exp. 31, 129–156. https://doi.org/10.14573/ALTEX.1403271.

Sörgel, F., Weissenbacher, R., Kinzig-Schippers, M., Hofmann, A., Illauer, M., Skott, A., Landersdorfer, C., 2002. Acrylamide: increased concentrations in homemade food and first evidence of its variable absorption from food, variable metabolism and placental and breast milk transfer in humans. Chemotherapy 48, 267–274. https://doi.org/10.1159/000069715.

Spînu, N., Cronin, M.T.D., Lao, J., Bal-Price, A., Campia, I., Enoch, S.J., Madden, J.C., Mora Lagares, L., Novič, M., Pamies, D., Scholz, S., Villeneuve, D.L., Worth, A.P., 2022. Probabilistic modelling of developmental neurotoxicity based on a simplified adverse outcome pathway network. Comput. Toxicol. 21, 100206 https://doi.org/10.1016/J.COMTOX.2021.100206.

Stadler, R.H., Blank, I., Varga, N., Robert, F., Hau, J., Guy, P.A., Robert, M.C., Riediker, S., 2002. Acrylamide from Maillard reaction products. Nature 6906 (419), 449–450. https://doi.org/10.1038/419449a.

Stephens, S.H., Logel, J., Barton, A., Franks, A., Schultz, J., Short, M., Dickenson, J., James, B., Fingerlin, T.E., Wagner, B., Hodgkinson, C., Graw, S., Ross, R.G., Freedman, R., Leonard, S., 2009. Association of the 5′-upstream regulatory region of the α7 nicotinic acetylcholine receptor subunit gene (CHRNA7) with schizophrenia. Schizophr. Res. 109, 102–112. https://doi.org/10.1016/J.SCHRES.2008.12.017.

Stiegler, N.V., Krug, A.K., Matt, F., Leist, M., 2011. Assessment of chemical-induced impairment of human neurite outgrowth by multiparametric live cell imaging in high-density cultures. Toxicol. Sci. 121, 73–87. https://doi.org/10.1093/TOXSCI/KFR034.

Strelau, J., Sullivan, A., Bottner, M., Lingor, P., Falkenstein, E., Suter-Crazzolara, C., Galter, D., Jaszai, J., Krieglstein, K., Unsicker, K., 2000. Growth/differentiation factor-15/macrophage inhibitory cytokine-1 is a novel trophic factor for midbrain dopaminergic neurons in vivo. J. Neurosci. 20, 8597–8603. https://doi.org/10.1523/JNEUROSCI.20-23-08597.2000.

Taleb, A., Lin, W., Xu, X., Zhang, G., Zhou, Q.G., Naveed, M., Meng, F., Fukunaga, K., Han, F., 2021. Emerging mechanisms of valproic acid-induced neurotoxic events in autism and its implications for pharmacological treatment. Biomed. Pharmacother. 137, 111322 https://doi.org/10.1016/J.BIOPHA.2021.111322.

Tau, G.Z., Peterson, B.S., 2010. Normal Development of Brain Circuits. Neuropsychopharmacology 1 (35), 147–168. https://doi.org/10.1038/npp.2009.115.

Turina, M., Mulhall, A., Gardner, S., Polk, H.C., Miller, F.N., 2008. Mannitol upregulates monocyte HLA-DR, monocyte and neutrophil CD11b, and inhibits neutrophil apoptosis. Inflammation 31, 74–83. https://doi.org/10.1007/S10753-007-9051-1.

Uehara, M., Yashiro, K., Mamiya, S., Nishino, J., Chambon, P., Dolle, P., Sakai, Y., 2007. CYP26A1 and CYP26C1 cooperatively regulate anterior-posterior patterning of the developing brain and the production of migratory cranial neural crest cells in the mouse. Dev. Biol. 302, 399–411. https://doi.org/10.1016/J.YDBIO.2006.09.045.

Van Battum, E.Y., Brignani, S., Pasterkamp, R.J., 2015. Axon guidance proteins in neurological disorders. Lancet Neurol. 14, 532–546. https://doi.org/10.1016/S1474-4422(14)70257-1.

Von Stedingk, H., Vikström, A.C., Rydberg, P., Pedersen, M., Nielsen, J.K.S., Segerbäck, D., Knudsen, L.E., Törnqvist, M., 2011. Analysis of hemoglobin adducts from acrylamide, glycidamide, and ethylene oxide in paired mother/cord blood samples from Denmark. Chem. Res. Toxicol. 24, 1957–1965. https://doi.org/10.1021/TX200284U.

Weiss, L.A., Arking, D.E., Daly, M.J., Chakravarti, A., Brune, C.W., West, K., O'Connor, A., Hilton, G., Tomlinson, R.L., West, A.B., Cook, E.H., Green, T., Chang, S.C., Gabriel, S., Gates, C., Hanson, E.M., Kirby, A., Korn, J., Kuruvilla, F., McCarroll, S., Morrow, E.M., Neale, B., Purcell, S., Sasanfar, R., Sougnez, C., Stevens, C., Altshuler, D., Gusella, J., Santangelo, S.L., Sklar, P., Tanzi, R., Anney, R., Bailey, A.J., Baird, G., Battaglia, A., Berney, T., Betancur, C., Bölte, S., Bolton, P.F., Brian, J., Bryson, S.E., Buxbaum, J.D., Cabrito, I., Cai, G., Cantor, R.M., Coon, H., Conroy, J., Correia, C., Corsello, C., Crawford, E.L., Cuccaro, M.L., Dawson, G., De Jonge, M., Devlin, B., Duketis, E., Ennis, S., Estes, A., Farrar, P., Fombonne, E., Freitag, C.M., Gallagher, L., Geschwind, D.H., Gilbert, J., Gill, M., Gillberg, C., Goldberg, J., Green, A., Green, J., Guter, S.J., Haines, J.L., Hallmayer, J.F., Hus, V., Klauck, S.M., Korvatska, O., Lamb, J.A., Laskawiec, M., Leboyer, M., Le Couteur, A., Leventha, B.L., Liu, X.Q., Lord, C., Lotspeich, L.J., Maestrini, E., Magalhaes, T., Mahoney, W., Mantoulan, C., McConachie, H., McDougle, C.J., McMahon, W.M., Marshall, C.R., Miller, J., Minshew, N.J., Monaco, A.P., Munson, J., Nurnberger, J.I., Oliveira, G., Pagnamenta, A., Papanikolaou, K., Parr, J.R., Paterson, A.D., Pericak-Vance, M.A., Pickles, A., Pinto, D., Piven, J., Posey, D.J., Poustka, A., Poustka, F., Regan, R., Reichert, J., Renshaw, K., Roberts, W., Roge, B., Rutter, M.L., Salt, J., Schellenberg, G.D., Scherer, S.W., Sheffield, V., Sutcliffe, J.S., Szatmari, P., Tansey, K., Thompson, A.P., Tsiantis, J., Van Engeland, H., Gates, A.M., Vieland, V. J., Volkmar, F., Wallace, S., Wassink, T.H., Wijsman, E.M., Wing, C., Wittemeyer, K., Yaspan, B.L., Zwaigenbaum, L., Yoo, S.Y., Hill, R.S., Mukaddes, S.M., Balkhy, S., Gascon, G., Al-Saad, S., Hashmi, A., Ware, J., Joseph, R.M., LeClair, E., Partlow, J.N., Barry, B., Walsh, C.A., Pauls, D., Moilanen, I., Ebeling, H., Mattila, M.L., Kuusikko, S., Jussila, K., Ignatius, J., Tolouei, A., Ghadami, M., Rostami, M., Hosseinipour, A., Valujerdi, M., Andresen, K., Winkloski, B., Haddad, S., Kunkel, L., Kohane, Z., Tran, T., Won Kong, S., O'Neil, S.B., Hundley, R., Holm, I., Peters, H., Baroni, E., Cangialose, A., Jackson, L., Albers, L., Becker, R., Bridgemohan, C., Friedman, S., Munir, K., Nazir, R., Palfrey, J., Schonwald, A., Simmons, E., Rappaport, L.A., Gauthier, J., Mottron, L., Joober, R., Rouleau, G., Rehnstrom, K., Von Wendt, L., Peltonen, L., 2009. A genome-wide linkage and association scan reveals novel loci for autism. Nature 7265 (461), 802–808. https://doi.org/10.1038/nature08490.

Widmer, F., Caroni, P., 1990. Identification, localization, and primary structure of CAP-23, a particle-bound cytosolic protein of early development. J. Cell Biol. 111, 3035–3047. https://doi.org/10.1083/JCB.111.6.3035.

Williams, N.M., Franke, B., Mick, E., Anney, R.J.L., Freitag, C.M., Gill, M., Thapar, A., O'Donovan, M.C., Owen, M.J., Holmans, P., Kent, L., Middleton, F., Zhang-James, Y., Liu, L., Meyer, J., Nguyen, T.T., Romanos, J., Romanos, M., Seitz, C., Renner, T.J., Walitza, S., Warnke, A., Palmason, H., Buitelaar, J., Rommelse, N., Vasquez, A.A., Hawi, Z., Langley, K., Sergeant, J., Steinhausen, H.C., Roeyers, H., Biederman, J., Zaharieva, I., Hakonarson, H., Elia, J., Lionel, A.C., Crosbie, J., Marshall, C.R., Schachar, R., Scherer, S.W., Todorov, A., Smalley, S.L., Loo, S., Nelson, S., Shtir, C., Asherson, P., Reif, A., Lesch, K.P., Faraone, S.V., 2012. Genome-wide analysis of copy number variants in attention deficit hyperactivity disorder: The role of rare variants and duplications at 15q13.3. Am. J. Psychiatry 169, 195–204. https://doi.org/10.1176/APPI.AJP.2011.11060822.

Xu, S., Li, M., Yang, C., Fang, X., Ye, M., Wei, L., Liu, J., Li, B., Gan, Y., Yang, B., Huang, W., Li, P., Meng, X., Wug, Y., Jiang, G., 2019. Altered functional connectivity in children with low-function autism spectrum disorders. Front. Neurosci. 13, 806. https://doi.org/10.3389/FNINS.2019.00806/BIBTEX.

Yang, Y., Paspalas, C.D., Jin, L.E., Picciotto, M.R., Arnsten, A.F.T., Wang, M., 2013. Nicotinic α7 receptors enhance NMDA cognitive circuits in dorsolateral prefrontal cortex. Proc. Natl. Acad. Sci. USA 110, 12078–12083. https://doi.org/10.1073/PNAS.1307849110/SUPPL_FILE/PNAS.201307849SI.PDF.

Yasui, D.H., Scoles, H.A., Horike, S.I., Meguro-Horike, M., Dunaway, K.W., Schroeder, D. I., Lasalle, J.M., 2011. 15q11.2–13.3 chromatin analysis reveals epigenetic regulation of CHRNA7 with deficiencies in Rett and autism brain. Hum. Mol. Genet. 20, 4311–4323. https://doi.org/10.1093/HMG/DDR357.

Zablotsky, B., Black, L.I., Maenner, M.J., Schieve, L.A., Danielson, M.L., Bitsko, R.H., Blumberg, S.J., Kogan, M.D., Boyle, C.A., 2019. Prevalence and Trends of Developmental Disabilities among Children in the United States: 2009-2017. Pediatrics 144. https://doi.org/10.1542/peds.2019-0811.